Atmos. Meas. Tech. Discuss., https://doi.org/10.5194/amt-2018-438
Manuscript under review for journal Atmos. Meas. Tech.
Discussion started: 17 December 2018

Atmospheric Measurement Techniques Discussions

Aerosol Optical Depth comparison between GAW-PFR and AERONET-Cimel radiometers from long term (2005-2015) 1-minute synchronous measurements

Emilio Cuevas[1], Pedro Miguel Romero-Campos[1], Natalia Kouremeti[2], Stelios Kazadzis[2], Rosa Delia García[3,1,4], Africa Barreto[5,1,4], Carmen Guirado-Fuentes[4,1], Ramón Ramos[1], Carlos Toledano[4], Fernando Almansa[5,1,4], and Julian Gröbner[2]

[1]Izaña Atmospheric Research Center (IARC), State Meteorological Agency (AEMET), Spain
[2]Physikalisch-Meteorologisches Observatorium Davos, World Radiation Center (PMOD/WRC), Davos, Switzerland
[3]Air Liquide España, Delegación Canarias, Candelaria, 38509, Spain
[4]Atmospheric Optics Group, Valladolid University, Valladolid, Spain
[5]Cimel Electronique, Paris, France

Correspondence: Emilio Cuevas
(ecuevasa@aemet.es)

Abstract.

A comprehensive comparison of more than 70000 synchronous 1-minute aerosol optical depth (AOD) data from three Global Atmosphere Watch-Precision Filter Radiometer (GAW-PFR) and 15 Aerosol Robotic Network-Cimel (AERONET-Cimel) radiometers was performed for the four nearby wavelengths (380, 440, 500 and 870 nm) in the period 2005-2015. The goal of this study is to assess whether, despite the marked differences between both networks and the number of instruments used, their long term AOD data are comparable and consistent. AOD traceability established by the World Meteorological Organization (WMO) consists in determining the percentage of synchronous data within specific limits. If, at least, 95 % of the AOD differences of an instrument compared to the WMO standards lie within these limits, both data populations are considered equivalent. The percentage of traceable data is 92.7 % (380 nm), 95.7 % (440 nm), 95.8 % (500 nm) and 98.0 % (870 nm). When small misalignments in GAW-PFR sun-pointing were fixed (period 2010-2015), the percentage of traceable data increased. The contribution of calibration related aspects to comparison outside the 95 % traceability limits is insignificant in all channels, except in 380 nm. The simultaneous failure of both cloud screening algorithms might occur only under the presence of cirrus, or altostratus clouds on the top of a dust-laden Saharan air layer. Differences in the calculation of the optical depth contribution due to Rayleigh scattering, and O_3 and NO_2 absorption have a negligible impact. For AOD > 0.1, a non-negligible percentage ($\sim$ 1.9 %) of the AOD data outside the 95 % traceability limits at 380 nm can be partly assigned to the different field of view of the instruments. The comparison of the Angström exponent (AE) shows that under non-pristine conditions (AOD > 0.03 and AE < 1) the AE differences remain < 0.1. The excellent traceability in this study has been obtained using well calibrated Master instruments.

Atmos. Meas. Tech. Discuss., https://doi.org/10.5194/amt-2018-438
Manuscript under review for journal Atmos. Meas. Tech.
Discussion started: 17 December 2018

Atmospheric Measurement Techniques Discussions

Copyright statement.

1 Introduction

In recent decades there has been a growing interest in the role played by atmospheric aerosols in the radiation budget and the Earth's hydrological cycle, mainly through their physical and optical properties (IPCC, 2013). The most comprehensive and important parameter that accounts for the optical activity of aerosols in the atmospheric column is the aerosol optical depth (AOD) (WMO, 2003, 2005). This is also a key parameter used in atmospheric column aerosol modelling (e.g. Basart et al., 2012; Benedetti et al., 2018; Cuevas et al., 2015; Huneeus et al., 2016) and in satellite observations (e.g. Sayer et al., 2012, 2013; Kahn and Gaitley, 2015). The second aerosol optical parameter in importance is the Angström exponent (Angstrom, 1929) that accounts for the spectral dependency of the AOD. Since the Angström exponent (AE) is inversely related to the average size of the aerosol particles, it is a qualitative indicator of the atmospheric aerosol particle size and therefore a useful parameter to assess the aerosol type (WMO, 2003).

At present, two global ground-based radiometer networks provide aerosol optical properties of the atmospheric column using centralized data processing procedures based on their respective standard criteria and also centralized protocols for calibration and quality control, linking all network instruments. These are AERONET-Cimel (AErosol RObotic NETwork - Cimel Electronique radiometer; http://aeronet.gsfc.nasa.gov; last access: 01 September 2018) and GAW-PFR (Global Atmospheric Watch - Precision Filter Radiometer; http://www.pmodwrc.ch/worcc/; last access: 05 September 2018) networks.

The World Optical Depth Research Calibration Center (WORCC) was established in 1996 at the Physikalisch Meteorologisches Observatorium Davos / World Radiation Center (PMOD / WRC (https://www.pmodwrc.ch/; last access: 25 June 2018). The GAW-PFR network (Wehrli, 2005) was initiated within PMOD/WRC for global and long-term atmospheric aerosol monitoring and accurate detection of trends. Aerosol data series measured at 12 core sites away from local and regional pollution sources, representative of atmospheric background conditions in different climates and environments of the planet, in addition to other 20 associated stations are included in this global network (Kazadzis et al., 2018a). For this reason, GAW-PFR uses the Precision Filter Radiometer (PFR), an accurate and reliable instrument regarding its absolute response stability over time that was designed for long term AOD measurements (Wehrli, 2008a). In 2006, the Commission for Instruments and Methods of Observation (CIMO) (WMO, 2007) recommended that the WORCC at the PMOD/WRC should be designated as the primary WMO Reference Centre for AOD measurements (WMO, 2005). The AERONET-Cimel network (Holben et al., 1998) was, in principal, designed to validate satellite products and to characterize the spatial-temporal distribution of atmospheric aerosols based on their optical properties. It is the largest surface-based aerosol global network with more than 25 sites with measurement series longer than 10 years and more than 150 sites having data sets > 5 years. Cimel radiometer data, part of AERONET, are processed centrally and freely delivered in near real time by the Goddard Space Flight Center.

Both networks, although designed to meet different objectives, are now global benchmarks for the study and characterization of aerosol optical properties worldwide, and for the evaluation of aerosol observations on board satellites and simulations with

Atmos. Meas. Tech. Discuss., https://doi.org/10.5194/amt-2018-438
Manuscript under review for journal Atmos. Meas. Tech.
Discussion started: 17 December 2018

models. Multiple studies have proliferated in recent years to obtain aerosol climatology and to determine AOD trends in different parts of the world (e.g. Nyeki et al., 2012; Klingmüller et al., 2016; Chedin et al., 2018).

However, these networks use radiometers with significant technical differences. Moreover, calibration methodologies, AOD calculation algorithms and data evaluation methods are also relatively different among the two networks. Since GAW-PFR is directly linked with WMO/CIMO, and AERONET is now the densest surface-based aerosol monitoring network and its results have been presented in numerous publications in the past 20 years, it is essential to assess to what extent AOD and Angström exponent (AE) from these networks are equivalent with each other. In addition, it is crucial to know the differences towards common homogenization activities among different instruments/networks measuring AOD.

The WMO has defined the GAW-PFR Triad as the world-wide reference for AOD measurements (WMO, 2005). Based on this concept, an instrument provides traceable measurements of AOD when this instrument can demonstrate an unbroken chain of calibrations between itself and the GAW-PFR Triad with AOD measurements within specified limits of the GAW-PFR reference. This can either be achieved by a direct comparison to the GAW-PFR Triad (Kazadzis et al., 2018a), or by using a portable transfer standard radiometer as it is presented in this study.

Several comparisons between AERONET-Cimel, GAW-PFR and other radiometers have been carried out in different places (Barreto et al., 2016; Kazadzis et al., 2014, 2018a; Kim et al., 2008; McArthur et al., 2003; Mitchell and Forgan, 2003; Nyeki et al., 2015; Schmid et al., 1999; Toledano et al., 2012). However, these comparisons have been performed during field intercomparison campaigns or during relatively short periods of time, so they are not representative of a large variety of atmospheric conditions. In addition, the type of instrument maintenance and the number and qualifications of staff serving them during campaigns is generally of a higher quality compared to that of the instrument daily operation in unattended mode. This might cause the instrument performance during intensive campaigns to be significantly better than that during operational mode.

The growing interest in the analysis of long-term AOD and AE data series for climatological purposes requires an assessment of their quality assurance and long-term intercomparability. GAW-PFR has a comprehensive calibration system (Kazadzis et al., 2018a; Schmid and Wehrli, 1995) that is transferred by a worldwide suite of reference instruments. However, AERONET-Cimel does not have a CIMO-WMO linked reference and is based on:

- Maintaining Master AERONET radiometers based on the Langley calibration technique at Izaña, Spain and Mauna Loa, USA.
- Calibration of all other instruments based on raw voltage ratios comparisons with Master instruments at dedicated sites (Carpentras-France, Washington DC-USA, Valladolid-Spain).

This is the first study to analyze the long-term traceability of AERONET-Cimel with respect to GAW-PFR, and therefore to assess the validity of the long AOD and AE AERONET-Cimel data series for climatological and climate change studies under specific quality control requirements.

There are few places in the world where synchronous observations of these two networks are available for long time periods in which a great variety of atmospheric turbidity conditions take place. The Izaña Observatory (IZO; Tenerife, the Canary

Islands) is one of them. The GAW-PFR measurements started at Izaña Observatory in 2001 (Wehrli, 2005) while AERONET-Cimel started in 2003 (Goloub et al., 2007). Since 2005, synchronous measurements (1-minute values), that have been evaluated following the calibration procedures of each of the networks, are available.

In addition, the Izaña Observatory is one of the two places in the world (the other is Mauna Loa - Hawaii, USA) where absolute sun-calibrations are performed using the Langley plot technique for both AERONET-Cimel and GAW-PFR reference instruments (Toledano et al., 2018) thanks to stable and very low AOD conditions during many days per year. Therefore, the instruments compared at the Izaña Observatory have been calibrated under the same environmental conditions, and therefore AOD differences can be directly linked with calibration principles, AOD post processing and other instrumental differences.

In this work, we analyze and evaluate the comparison of 11 years (2005-2015) of 1-minute synchronous observations of AOD with AERONET-Cimel and GAW-PFR in four common or near wavelengths, assessing the results and explaining the possible causes of these differences. Some preliminary technical details on the traceability between GAW-PFR and AERONET-Cimel were reported in a technical report by Romero-Campos et al. (2017).

In Section 2 the facility in which this long-term comparison has been carried out is described. The technical characteristics of the AERONET-Cimel and GAW-PFR instruments are provided in Section 3, with special emphasis on the technical and methodological differences of both networks. Section 4 describes the methodology followed in this intercomparison based on the concept of WMO-GAW traceability. Results are given in Section 5. A summary and conclusions are provided in Section 6.

2 Site Description

IZO (28.3° N, 16.5° W; 2373 m a.s.l.) is located in Tenerife (Canary Islands, Spain) and is managed by the Izaña Atmospheric Research Center (IARC) which is part of the State Meteorological Agency of Spain (AEMET). It is a suitable place for long-term studies of aerosol optical properties under quite contrasting atmospheric and meteorological conditions. This is because IZO is located in the free troposphere (FT) above the temperature inversion caused by the trade wind regime in lower levels and general subsidence associated to the branch of the decay of Hadley's cell aloft (Carrillo et al., 2016). This meteorological feature favours, during most of the year, the presence of pristine skies and clean air representative of atmospheric background conditions (Cuevas et al., 2013; Rodríguez et al., 2009). On the other hand, its proximity to the African continent makes it a privileged site for observing and characterizing the Saharan Air Layer (SAL) that normally presents a high burden of desert mineral dust, especially during the summer months (Basart et al., 2009; Rodríguez et al., 2011; Cuevas et al., 2015). At this time of the year, the SAL impacts the subtropical free troposphere over the North Atlantic with large interannual (Rodríguez et al., 2015) and sharp intraseasonal (Cuevas et al., 2017a) variability.

The contrasting atmospheric conditions that occur at IZO allow the comparison of the two networks, which can be performed under a wide range of AOD values. Mostly for pristine conditions (AOD $\leq$ 0.03) but also for relatively high turbidity (AOD > 0.6) linked with dust aerosol related intrusions. In addition, the location offers the possibility of observing rapid changes in AOD, going from pristine conditions to dusty skies, and viceversa, in a matter of a few hours, especially in the summer

Atmos. Meas. Tech. Discuss., https://doi.org/10.5194/amt-2018-438
Manuscript under review for journal Atmos. Meas. Tech.
Discussion started: 17 December 2018

Atmospheric Measurement Techniques Discussions

period. This defines IZO as a good atmospheric aerosol natural laboratory to compare the performance of different radiometers measuring AOD.

The privileged conditions of pristine skies that characterize IZO during many days a year have allowed this observatory to become a calibration site for the GAW-PFR and AERONET-Cimel networks since 2001 and 2003, respectively, where the extraterrestrial constants are determined with direct sun observations using the Langley plot technique (Toledano et al., 2018). In addition, since July 2014, IZO has also been designated by the WMO as a CIMO testbed for aerosols and water vapour remote sensing instruments. IZO is a station of the Baseline Surface Radiation Network (Driemel et al., 2018; García et al., 2018)). Details of the IZO facilities, measurement programmes and main results can be found in Cuevas et al. (2017b).

3 GAW-PFR and AERONET-Cimel radiometers

The two types of radiometers intercompared in this study are Cimel CE318-N (Holben et al., 1998), hereinafter referred to as Cimel, the standard instrument of AERONET until the recent appearance of CE318-T (Barreto et al., 2016), and the Precision Filter Radiometer (Wehrli, 2005) standard instrument of the GAW-PFR network. The main features of these two radiometers are described in Table 1.

The Cimel (Holben et al., 1994, 1998) is a radiometer equipped with a 2-axis robot that performs two types of basic radiation measurements: direct solar irradiance and sky (radiance) observations, thanks to an automatic pointing robot that executes the observation sequences that have been scheduled. The field of view (FOV) of the instrument is 1.2°. The wavelengths in which the measurements are sequentially made by a single detector depend on the interference filters that each version of the radiometer has installed in the filter wheel, which is located inside the sensor head and which is moved by a stepper motor. The Cimel versions used in this study have at least eight interference filters centred at 340, 380, 440, 500, 675, 870, 940, and 1020 nm and 10 nm full width at half maximum (FWHM) bandwidth, except for 340 and 380 nm which have 2 and 4 nm FWHM, respectively. Solar irradiance is measured with a Silicon detector in these channels. The possible deterioration of the interference filters is minimized since they are only sun-exposed during programmed direct-sun measurements, which last $\sim$ 1 second per channel, while the rest of the time the Cimel is taking sky radiance measurements, or at rest position, looking downwards.

The PFR (Wehrli, 2000, 2005, 2008a, b)is designed for continuous and automated operation under a broad range of weather conditions. It accurately measures direct solar radiation transmitted in four independent narrow channels centred at 368, 412, 500 and 862 nm, with 5 nm FWHM bandwidth. The FOV of the instrument is 2.5°. Dielectric interference filters manufactured by ion-assisted-deposition technique are used to assure significant larger stability in comparison to the one manufactured by classic soft-coatings. The PFR was designed for long-term stable measurements, therefore the instrument is hermetically sealed with an internal atmosphere slightly pressurized (2000 hPa) with dry nitrogen, and is stabilized in temperature with a Peltier-type thermostatic system maintaining the temperature of the detector head at 20° C $\pm$ 0.5° C. So, this system makes corrections of the sensitivity for temperature unnecessary, and also prevents accelerated ageing of filters, ensuring the high stability of the PFR. The PFR has been selected by the WMO as the reference instrument for long-term AOD observations. The PFR is

Atmos. Meas. Tech. Discuss., https://doi.org/10.5194/amt-2018-438
Manuscript under review for journal Atmos. Meas. Tech.
Discussion started: 17 December 2018

Atmospheric Measurement Techniques Discussions

mounted on a sun tracker, pointing always at the sun without any active optimization of the position, The detectors are only exposed for a short time periods, since an automated shutter opens every minute for 10s for sun measurements, minimizing degradation related with the filters exposure.

The expected uncertainty of AOD in the four channels of the PFR radiometer is from 0.004 (862 nm) up to 0.01 (368 nm) (Wehrli, 2000). For Cimel radiometer, the expected uncertainty of level 2-AOD product is found between 0.002 and 0.005, larger for shorter wavelengths for Masters, and between 0.01 and 0.02, larger in the UV, for field instruments, under conditions of clear skies (Eck et al., 1999; Barreto et al., 2016).

In relation to the calibration of both networks, GAW and AERONET, they use high mountain stations with very stable and low AOD over a day in which consecutive measurements can be performed over a wide range of optical air mass (approximately between 2 and 5) in the shortest possible time, in order to calibrate Masters using the Langley plot technique. These calibrations are subsequently transferred to the field instruments of the network in other sites through regular intercomparison campaigns, in the case of the AERONET-Cimel and to the reference PFR triad maintained at PMOD/WRC for the GAW-PFRs.

IZO is one of the two sites of absolute calibration of both networks, which represents an advantage when comparing the two instruments, eliminating, to a large extent, errors caused by the calibration transfer. However, there are differences between the calibration methodologies used by both networks. AERONET obtains the calibration by means of the average of a few extra-terrestrial V_o constants, obtained from Langleys, performed in a relatively short time (3-4 months). However, GAW obtains the calibration by means of the temporal lineal fit to a larger number of extra-terrestrial constants V0 obtained from Langley plots performed during 6 months (Wehrli, 2000; Kazadzis et al., 2018a). Details on requirements for performing Langley calibrations of Master instruments by GAW and AERONET, and their uncertainties, are analyzed in detail by Toledano et al. (2018).

4 Data and methodology used in this study

The AOD at each wavelength is obtained from the Beer-Bouguer-Lambert law for radiometers collecting spectral direct sun measurements.

$$I(\lambda) = I_0(\lambda)\exp(-\tau m) \quad (1)$$

where $I(\lambda) is the direct sun signal at ground level at wavelength \lambda$, $I_0(\lambda)$ is the extraterrestrial signal of the instrument corrected by the Earth-Sun distance, and m is the optical air mass in the measurement path (Kasten and Young, 1989).

The AOD comparison has been performed using 1-minute synchronous data from the four closest channels of both instruments in the period 2005-2015 (more than 70000 data-pairs in each channel). Thus, in the case of GAW-PFR, the four available channels of 368, 412, 500 and 862 nm were analyzed, while in the case of AERONET-Cimel, only the 380, 440, 500 and 870 nm channels were considered (Table 1). For the 500 nm channel, the differences between nominal wavelengths of both networks differ by a maximum of 1.8 nm. However, the differences in nominal wavelengths in the rest of the compared channels present higher differences. Therefore, the AOD values of the original GAW-PFR 368, 412 and 862 nm channels have been extrapolated to the corresponding AERONET-Cimel channels (380, 440 and 870 nm) using the Angström power law, and the GAW-PFR AE calculated from the four PFR AOD measurements.

Atmos. Meas. Tech. Discuss., https://doi.org/10.5194/amt-2018-438
Manuscript under review for journal Atmos. Meas. Tech.
Discussion started: 17 December 2018

Atmospheric Measurement Techniques Discussions

Table 1. Main features of the GAW-PFR and AERONET-Cimel radiometers.

	GAW-PFR	**AERONET-Cimel**
Type of instrument	Standard version Field instrument	Standard version Master instrument
Type of observation	Automatic continuous direct sun irradiance	Automatic sun-sky tracking
Available standar channels	368,412,500,862 nm	340,380,440,500,675,870,1020,1640 nm
FWHM	5 nm	2nm(340nm), 4nm(380nm), 10nm(VIS-NIR), 25nm(1640nm)
AOD uncertainty	$\pm$ 0.01	$\pm$ 0.005 (Master instruments)
FOV (FWHM)	2.5° (1.2° plateau, 0.7° slope)	1.2°
Sun tracker	No specific Sun tracker	Sun tracker robot specifically designed by Cimel
Temperature control	Temperature controlled 20°C$\pm$0.5°C	Temperature correction is applied
Power	Grid	Solar panels/grid
Data transmission	Local PC FTP	Local PC FTP Satellite transmission
Calibration	In situ long-term Langley plots/traceability with reference triad	2-3 months Langleys plots

A total of three GAW-PFR and 15 AERONET-Cimel instruments have participated in this intercomparison study covering the period 2005-2015. Their corresponding reference numbers are shown in Table 2.

The data matching in our comparison analysis was performed with synchronous 1-minute AOD values of both networks labelled with QC flags that guarantee proven quality data not affected by the presence of clouds. In the case of the GAW-PFR network (Wehrli, 2008a) the flags take the value 0 (cloudless conditions, no wavelength crossings and sun pointing within certain limits, more details in Kazadzis et al. (2018a)) for all those selected records. In the case of the AERONET-Cimel network, the selected AOD data are Level 2 data, which have been cloud filtered by the Smirnov algorithm (Smirnov et al., 2000) based on the triplet method, and visually screened. Level 2 AERONET AOD data corresponds to version 2 of the algorithm which has been, until recently, the most updated version available in AERONET. Recently, version 3 has just been introduced (Giles et al., 2018). Since a huge amount of published results are based on AERONET V2, a detailed comparison assessment between AERONET V2 and V3 must be presented before comparing AERONET V3 AOD with GAW-PFR.

GAW-PFR and AERONET-Cimel instruments use the same time reference. The synchronization between PC and GAW-PFR data-logger was performed every 12 hours since 2005, being improved to 6 hours after 2013 using NTP servers via Internet. From 2005 to 2012 the time of the AERONET-Cimel Masters was checked manually once per day using a handheld GPS. From 2012 onwards, the time was adjusted automatically 3 times per day using the ASTWIN Cimel software. In turn, the PC time is adjusted through the AEMET internal time server every 15 minutes.

Atmos. Meas. Tech. Discuss., https://doi.org/10.5194/amt-2018-438
Manuscript under review for journal Atmos. Meas. Tech.
Discussion started: 17 December 2018

Atmospheric Measurement Techniques Discussions

Table 2. GAW-PFR and AERONET-Cimel instrument numbers used in this study in the period 2005-2015.

Instruments used in this study	Period 2005-2009	Period 2010-2015
GAW-PFR	2 instruments: #6,#25	2 instruments: #6,#21
AERONET-Cimel	13 instruments: #25,#44,#45,#79,#117,#140 #244,#245,#380,#382,#383,#398,#421	5 instruments: #244, #347, #380 #421, #548

GAW-PFR provides AOD values every 1 minute as an average of 10 sequential measurements of total duration less than 1 second, while AERONET-Cimel provides AOD values every 15 minutes (from 3 measurements separated by 30 seconds). We consider synchronous 1-minute data when GAW-PFR and AERONET-Cimel AOD data were obtained with a difference of $\sim$ 30 s.

The criterium for traceability used in this study follows the recommendation of the WMO (WMO, 2005) which states that 95% of the AOD measurements fall within the specified acceptance limits, taking the GAW-PFR as reference:

$$U_{95} = \pm(0.005 + 0.010/m) \tag{2}$$

where m is the optical air mass.

The acceptance limits proposed by WMO take into account, on the one hand, the uncertainty inherent in the calculations of the AOD, and on the other, the uncertainty associated with the calibration of the instrument. The latter, for the case of instruments with finite field of view direct transmissions, such as the PFR and the Cimel, is dominated by the influence of the top-of-the-atmosphere signal determined by Langley plot measured, divided by the optical air mass.

The first term of Eq. 2 (0.005) represents the maximum desirable uncertainty due to the atmospheric parameters used for the AOD calculation (additional atmospheric trace gas corrections, and Rayleigh scattering). The second term describes calibration related relative uncertainties which scale therefore with the inverse of air mass. The WMO recommends an upper limit for the calibration uncertainty of 1%.

Synchronous AE data provided by both instruments have also been compared. GAW-PFR determines AE using all four PFR wavelengths (Nyeki et al., 2015), while AERONET-Cimel uses different pairs of wavelengths (340-440, 380-500, 440-675, 440-870, 500-870 nm) (Holben et al., 1998). As a consequence, we have calculated a new AE for the Cimel radiometer using the four channels equivalent to those of the PFR.

A first simple approach to calculate the circumsolar radiation of each radiometer taking into account their respective FOVs, AOD, total O_3 and pressure values, has been performed with the SMARTS (Simple Model of the Atmospheric Radiative Transfer of Sunshine) model version 2.9.5 (Gueymard, 1995). This spectral model, that covers the UVA, UVB, Visible and Near-Infrared bands, can be used to simulate the spectral irradiance that would be measured by a spectroradiometer (Gueymard, 2001). This model, which has been used and compared with LibRadtran for determining circumsolar radiation (Eissa et al., 2015) is used in this study to estimate, in a first approximation, the differences in AOD caused by the different FOV of PFR and Cimel radiometers.

Atmos. Meas. Tech. Discuss., https://doi.org/10.5194/amt-2018-438
Manuscript under review for journal Atmos. Meas. Tech.
Discussion started: 17 December 2018

Atmospheric Measurement Techniques Discussions

5 Results

5.1 AERONET-Cimel AOD traceability

The analysis shows that the AOD from AERONET-Cimel radiometers meet the WMO traceability criteria in all four common wavelength channels. The lowest agreement is found in the UV channel (380 nm) with 92.7 % of the minute average data, and the highest in the infrared channel (870 nm) with 98.0 % (Figure 1; Table 4).

However, in the first half of the comparison period (2005-2010) there was a number of mechanical problems in the solar tracker where the GAW-PFR was mounted on, which caused frequent problems of sun pointing. This finding was confirmed with data from the four–quadrant silicon detector (Wehrli, 2008a) that showed diurnal variation of the PFR sensors position up to 0.3°, and relatively poor long term stability.

From 2010 onwards, the PFR was mounted on an upgraded solar tracker of higher performance and precision. This helped to reduce problems in sun pointing, that were the main cause of AOD discrepancies between PFR and Cimel, and therefore not attributable to the instruments themselves.

In addition, since 2010, Cimel #244 has been in continuous operation most of the time at the Izaña AERONET station, greatly simplifying calibration procedures and the corresponding data evaluation. During the 2010-2015 period, the fraction of traceable AOD measurements of the total between the AERONET-Cimel radiometer and the GAW-PFR improves to 93.46 % in the 380 nm channel, and this percentage rises to 99.07 % for the 870 nm channel. We must clarify that this improvement is mostly due to the upgraded solar tracker used with the PFR since 2010.

Despite the technical differences between both radiometers, described above, and the different calibration protocols, cloud-screening algorithms and data processing procedures, the data series of both instruments, can be considered as equivalent, except for 380 nm, according to the WMO traceability criteria defined previously (Eq. 2). This explains the excellent agreement in the long-term AOD climatology shown for GAW-PFR and AERONET-Cimel in Toledano et al. (2018).

In order to confirm the appropriateness of performing the AOD comparison in common channels by interpolating those of the GAW-PFR to those of AERONET-Cimel, we have compared the percentages of AERONET-Cimel AOD data meeting the WMO criteria for the four interpolated GAW-PFR channels with those using the original GAW-PFR channels (Table 3). For shorter wavelengths, the percentage of data within the WMO limits decreases when the original GAW-PFR channels are used as a reference, mainly, and as expected, in the 412 nm channel as this differs considerably from the nominal value of the corresponding AERONET-Cimel channel (440 nm). For 500 nm and 870/862 nm there are no significant differences. Hereinafter, in this study the interpolated GAW-PFR channels are used.

A more detailed statistical evaluation for different scenarios of aerosol loading (three ranges of AOD) and aerosol size (three ranges of AE) for each compared channel has been performed (see Table 4). We can see that the poorest agreement is obtained at the shorter wavelength channels (440 nm, and especially 380 nm).

Kazadzis et al. (2018b) also found a decrease in the percentage of AOD meeting the WMO criteria for 368 nm and 412 nm spectral bands during the Fourth WMO Filter Radiometer Comparison for aerosol optical depth measurements. As these authors pointed out, the shorter the wavelength, the poorer the agreement because of several reasons: AOD in the UV suffers from out-

Atmos. Meas. Tech. Discuss., https://doi.org/10.5194/amt-2018-438
Manuscript under review for journal Atmos. Meas. Tech.
Discussion started: 17 December 2018

Atmospheric Measurement Techniques Discussions

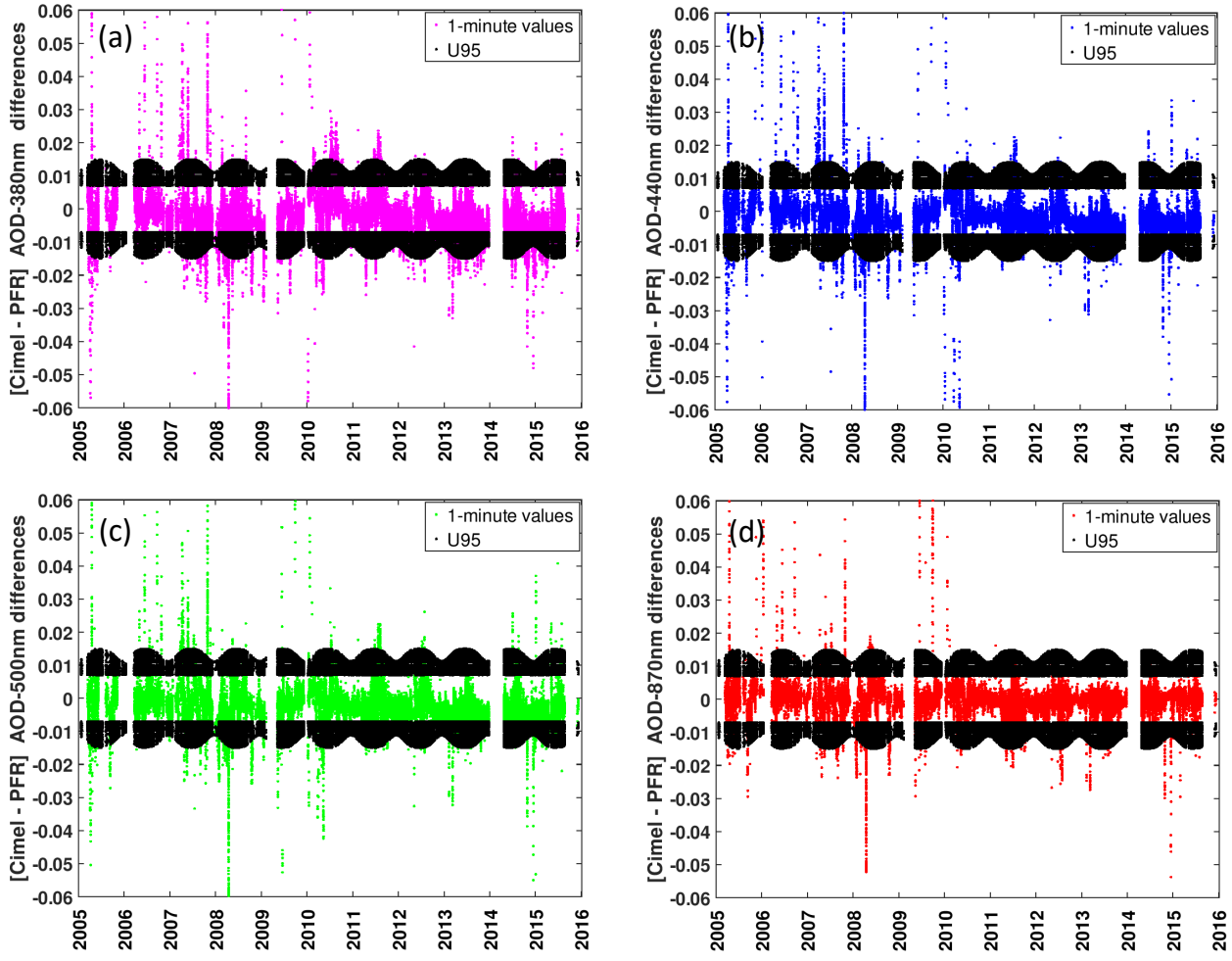

Figure 1. 1-minute AOD data differences between AERONET-Cimel and GAW-PFR for (a) 380 nm (70838 data-pairs), (b) 440 nm (71645 data-pairs), (c) 500 nm (70833 data-pairs) and (d) 870 nm (71660 data-pairs) for the period 2005-2015. Black dots correspond to the $U95$ limits. Some outliers are out of the ∼0.06 AOD differences range.

Table 3. Percentage of AERONET-Cimel AOD meeting the WMO criteria for the four interpolated, and original GAW-PFR channels.

Interpolated GAW-PFR channel (%)	Original GAW-PFR channel (%)
380 nm (92.7)	368 nm (91.1)
440 nm (95.7)	412 nm (92.8)
500 nm (95.8)	500 nm (96.3)
870 nm (98.0)	862 nm (97.8)

Atmos. Meas. Tech. Discuss., https://doi.org/10.5194/amt-2018-438
Manuscript under review for journal Atmos. Meas. Tech.
Discussion started: 17 December 2018

Atmospheric Measurement Techniques Discussions

Table 4. Percentage of AERONET-Cimel AOD data meeting the WMO criteria for the four compared channels, and different AOD and AE scenarios for the period 2005-2015. Last row corresponds to the total percentages for the sub-period 2010-2015. In bold, AOD and AE traceability is > 95%.

% of data within WMO limits	380 nm	440 nm	500 nm	870 nm
AOD≤0.05	94.4	**96.8**	**97.0**	**98.5**
0.05<AOD≤0.10	91.0	93.1	92.0	94.2
AOD>0.10	75.0	86.5	92.0	**95.9**
AE≤0.3	76.4	85.9	92.0	**96.6**
0.3<AE≤0.7	93.8	**96.9**	**96.5**	**97.9**
AE>0.7	94.9	**97.1**	**97.3**	**98.9**
Total 2005-2015	92.7	**95.7**	**95.8**	**98.0**
Total 2010-2015	93.5	**97.4**	**97.2**	**99.1**

of-band or at least different blocking of the filters, small differences in central wavelength or FWHM have larger impact, the Rayleigh correction is more critical, and NO_2 absorptions are treated differently. Regarding the effect of the aerosol load and particle size on the AOD differences, our results confirm the decrease of agreement between the two instruments for very large particles coincident with almost pure dust (AE $\leq$ 0.3), and high turbidity conditions (AOD > 0.1). A similar result was reported by Kim et al. (2008), who attributed these discrepancies to the possible spatial and temporal variability of aerosols under larger optical depths in addition to the effect of the different FOV of both radiometers. In our case, and according to previous studies on AOD climatology at IZO (Barreto et al., 2014), the presence of high mineral dust burden when the station is within the SAL, does not necessarily imply lower atmospheric stability conditions. For these reasons, we assumed that the different FOV of these instruments can be one of the main causes of part of the AOD 1-minute differences outside the U95 limits, under high AOD conditions. This issue is specifically addressed in Section 5.4.

In general, the agreement obtained with the 1-minute AOD data is slightly lower than that obtained during short campaigns, such as those reported by (Kazadzis et al., 2014) at Athens observatory (465 data-pairs), and Barreto et al. (2016) at Izaña Observatory (5566 data-pairs), with agreements > 99 % for AOD_{870nm} and AOD_{500nm} in case of Barreto et al. (2016). However, our results for AOD_{500nm} (> 95 % of 70833 data-pairs) is significantly better that that observed by Kazadzis et al. (2014) ($\sim$ 48 % of 465 data-pairs) covering a relatively short range of AOD. The probable cause for the poor agreement found by (Kazadzis et al., 2014) was a poor calibration in the 500 nm channel in at least one of the instruments operating at Athens.

In addition, short-term campaigns usually cover a small range of AOD, normally with low AOD, and instruments are carefully and frequently supervised. On the contrary, during our intercomparison over a period of 11 years, the operation of the instruments can be described much more as the normal operation of such a system for a long term period of measurements, than that of intensively attended instrumentation during short period intercomparison campaigns.

An interesting aspect of this study is that it is not a simple intercomparison exercise among two instruments but a comparison of a number of instruments that acted as references or masters for the AERONET/Europe Network.

Atmos. Meas. Tech. Discuss., https://doi.org/10.5194/amt-2018-438
Manuscript under review for journal Atmos. Meas. Tech.
Discussion started: 17 December 2018

Atmospheric Measurement Techniques Discussions

Table 5. Basic skill-scores from the AOD intercomparison between GAW-PFR and AERONET-Cimel for the period 2005-2015. The skill scores definitions are found in Huijnen and Eskes (2012).

Period	2005-2015			
Wavelengths (nm)	380	440	500	870
Mean Bias (MB)	0.0026	0.0018	0.0021	0.0001
Modified Normalized Mean Bias (MNMB)	0.1301	0.1046	0.1474	0.0129
Fractional Gross Error (FGE)	0.1727	0.1546	0.1918	0.1837
Root Mean Square Error (RMSE)	0.0081	0.0070	0.0064	0.0049
Pearson's correlation coefficient (r)	0.9910	0.9925	0.9939	0.9949
Number of data-pairs	70838	71645	70833	71660

In the first period (2005-2009), a total of 13 Cimel radiometers were used, while in the second period (2010-2015), five Cimel radiometers have participated, and for much of this period, the Cimel #244 was operating as the permanent AERONET reference instrument at IZO. Once the most important causes of non-traceability in the first period were ruled out, which were associated with a poor pointing of GAW-PFR due to problems in the sun-tracker, we can conclude that there are no significant differences in the percentages of traceable data of both periods. This means that the continuous change of Master Cimel instruments used in the 2005-2010 period did not have a significant impact on AOD data comparison differences. This proves the consistency and homogeneity of the long AERONET-Cimel AOD data series, and their comparability with the GAW-PFR AOD data series, regardless of the number of instruments used to generate these data series.

In our study, with a number of comparison data-pairs one or two orders of magnitude higher than those used in short campaigns, the results shown in Table 4 can be considered excellent. In addition to the traceability scores, we have introduced some basic skill scores corresponding to the AOD intercomparison between GAW-PFR and AERONET-Cimel for the period 2005-2015 (Table 5) to be in line with previous studies that have performed short-term comparisons between these two instruments. The definitions of the used skill scores can be found in Huijnen and Eskes (2012).

The Pearson's correlation coefficient (r) values of the PFR-Cimel 1-minute AOD data-pairs, are higher than 0.99 in all channels. Concerning Mean Bias (MB) and Root Mean Square Error (RMSE) associated to AOD differences, our results show quite similar skill scores to those found at Mauna Loa, USA for AOD_{500nm} (Kim et al., 2008), although the number of data-pairs used at Izaña Observatory (∼71000) is much higher than that of Mauna Loa (∼9700), and the AOD range of our study is much larger than that of the comparison performed in Mauna Loa. Kim et al. (2008) summarize results of previous short-term intensive studies (McArthur et al., 2003; Mitchell and Forgan, 2003; Kim et al., 2005; Schmid et al., 1999) carried out in stations where the radiometers were calibrated by intercomparison with Master or reference instruments. These results show MB values to be within 0.01 bias, one order of magnitude lower than in Mauna Loa and Izaña Observatories, highlighting the importance of having well calibrated instruments to carry out these type of comparisons.

For the period 2010-2015 (not shown here), and as expected, the RMSE and the Pearson's correlation improve slightly compared with the whole period 2005-2015.

Atmos. Meas. Tech. Discuss., https://doi.org/10.5194/amt-2018-438
Manuscript under review for journal Atmos. Meas. Tech.
Discussion started: 17 December 2018

5.2 Non-traceability assessment

The interpolation of the CIMEL AODs to the PFR AOD wavelengths can be one of the sources of uncertainty in this comparison assessment. The greatest uncertainty arises in the extrapolation of the 412 nm PFR to retrieve AODs at the CIMEL AOD_{440nm}. Using the Angström formula we have calculated that for an uncertainty of ± 0.5 in the Angström exponent and for AOD of 0.1 at 412 nm, the introduced uncertainty is of the order of ± 0.003, while for an AOD_{412nm} of 0.5 and an AE uncertainty of ± 0.3, the introduced uncertainty is ± 0.008. For all other AOD interpolations the errors are smaller.

5.2.1 Calibration related errors

The calibration procedures of the AERONET-Cimel and GAW-PFR radiometers are different. While in the case of GAW-PFR, frequent calibrations are established throughout the year and the calibration value is linearly interpolated in time, in AERONET-Cimel a constant calibration value is assumed in the intermediate period between two consecutive calibrations carried out on an annual basis.

A not sufficiently accurate determination of the calibration constant results in a fictitious AOD diurnal evolution presenting a concave or convex characteristic curve due to the calibration error dependence on solar air mass. The largest error occurs in the central part of the day (or lower air masses), mainly, in clean days with very low aerosol load (< 0.02 in 500 nm), as reported by Romero and Cuevas (2002) and Cachorro et al. (2004).

However, in this work we have used data from Master instruments (in-situ absolute calibration) in the case of AERONET-Cimel, and field instruments with in-situ Langley calibrations and direct traceability to the reference triad, in the case of GAW-PFR. The typical calibration uncertainty for a single Langley plot is 0.7-0.9 % (at the 95 % confidence level), and it is reduced to 0.4 % in the case of Izaña Observatory when averaging at least 10 Langley-derived extraterrestrial constants which is the normal procedure (Toledano et al., 2018). Moreover, in our case, we rule out additional calibration uncertainties introduced by calibration constants transfer at least for the Cimel instruments. Considering the PFRs operated at IZO, a direct yearly comparison of the Langley based V_o's with the reference triad at PMOD/WRC showed differences lower than 1 % for all channels for the 2005-2015 period.

Since possible calibration errors would result in higher AOD differences in lower optical air masses (based on Eq. 2), we have represented the AOD differences between GAW-PFR and AERONET-Cimel versus optical air mass for the four channels under pristine conditions ($AOD_{500nm} \leq 0.03$). Although calibration inaccuracies affect all channels, they are especially well observable at shorter wavelengths (Figure 2).

The total percentage of AOD traceable data pairs under pristine conditions ($AOD_{500nm} \leq 0.03$) is very high for all wavelengths (> 97.9 %) falling within the $U95$ limits (Table 6), except for 380 nm.

There is no dependence on 1-minute AOD differences with optical air mass for 440, 500 and 870 nm, and a slight dependence for 380 nm (Table 6) with lower traceability at lower optical air masses.

The percentage of AOD traceable data is almost the same regardless of the optical air mass interval for 440, 500 and 870 nm. So, ∼1.5 % of the 1-minute AOD data-pairs do not meet the WMO criteria for pristine conditions regardless of the

Atmos. Meas. Tech. Discuss., https://doi.org/10.5194/amt-2018-438
Manuscript under review for journal Atmos. Meas. Tech.
Discussion started: 17 December 2018

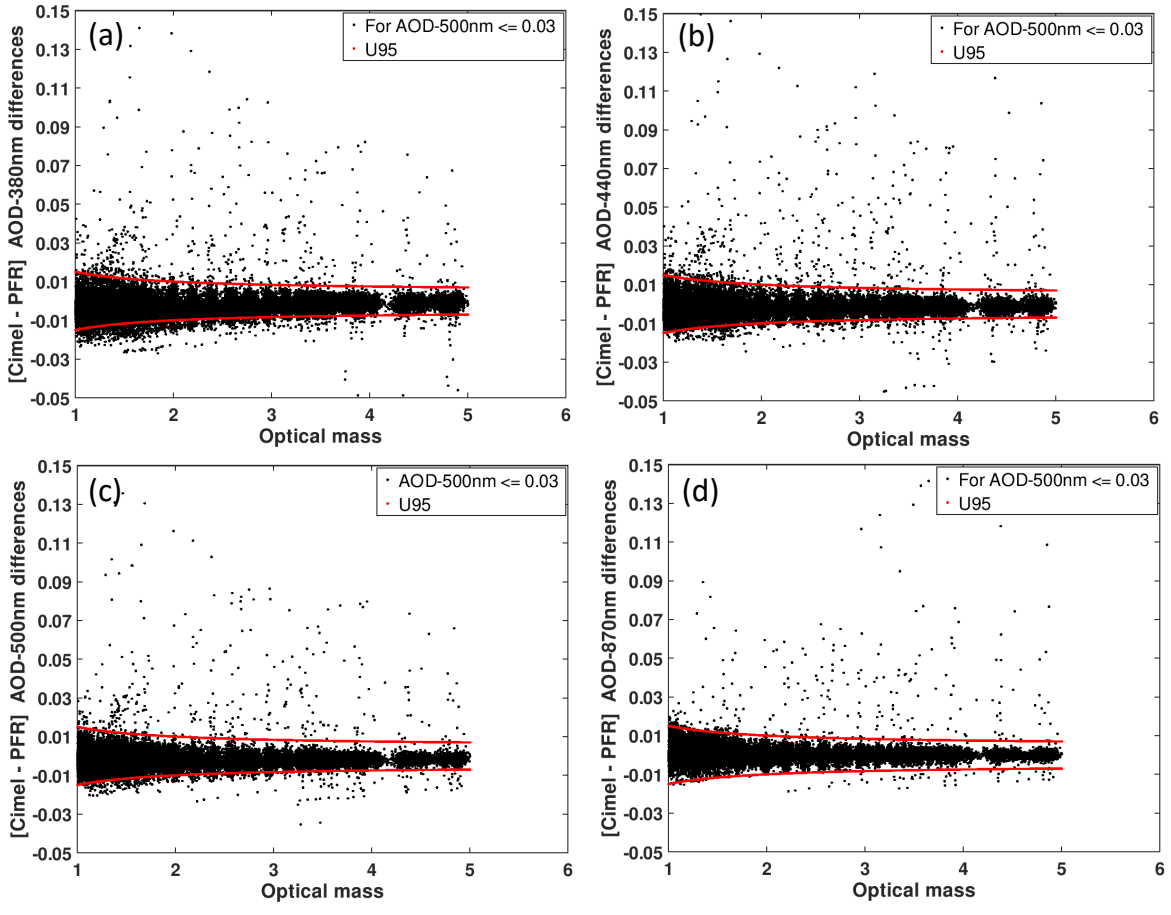

Figure 2. 1-minute AOD differences between GAW-PFR and AERONET-Cimel versus optical air mass (m) under pristine conditions ($AOD_{500nm} \leq 0.03$) in the period 2005-2015 for (a) 380 nm, (b) 440 nm, (c) 500 nm and (d) and 870 nm.

Table 6. Percentage of 1-minute AOD data meeting the WMO criteria for each wavelength for different optical air mass intervals under pristine conditions ($AOD_{500nm} \leq 0.03$) in the period 2005-2015.

Traceability for $AOD_{500nm} \leq 0.03$	Total (%)	$1 \leq m \leq 2$ (%)	$2 \leq m \leq 3$ (%)	$3 \leq m \leq 4$ (%)	$4 \leq m \leq 5$ (%)
380 nm	95.8	94.5	96.0	97.4	97.2
440 nm	97.9	97.9	97.7	98.2	97.7
500 nm	98.3	98.4	98.1	98.6	98.4
870 nm	99.2	99.4	99.3	99.2	98.6

airmass. Taking account of all of the above we can conclude that non-traceability caused by calibration uncertainty might be considered as negligible (or less than 1 %) for these channels. Most of the differences outside the U95 limits for very low AOD values, could be due to instrumental noise. It should be noted that although the few outliers are evenly distributed throughout the airmass range, they are not equally distributed with respect to the zero of the AOD difference, but there is a bias with positive large outliers (higher Cimel AOD), already reported by Nyeki et al. (2013), and small negative outliers for optical air mass lower than 2. These outliers can be explained by several causes such as cloud contamination, dirtiness, condensation on lenses, presence of small insects on the optics outside, etc. The correct cause attribution of each outlier would require manual inspection and additional maintenance information that is not available. However, we suggest that this is not crucial because these outliers represent a very small percentage of the data, as shown in Table 6.

However, for 380 nm the percentage of non-traceable values increases by 1.4 % from $1 \leq m < 2$ to $4 \leq m < 5$. This result is consistent with the fact that the greatest uncertainty in the determination of the calibration constants is observed in the UV range, and the lowest uncertainty in the near-infrared channel (Toledano et al., 2018). We also have to consider that other AOD retrieval input uncertainties are air mass dependent, such as Rayleigh related optical thickness.

We investigated more in detail whether the outliers were predominantly caused by one of the two instruments. Since, as explained above, a not very accurate calibration results in a pronounced diurnal AOD curvature (Romero and Cuevas, 2002; Cachorro et al., 2004). According to Cachorro et al. (2004, 2008) fictitious differences of up to 0.06 between the minimum and the maximum AOD can be recorded in a day with constant AOD as a result of a non-accurate calibration or not cleaned instruments. Certainly, the amplitude of the diurnal differences depends on the calibration factor. Thus, we have calculated for the non-traceable AOD data the diurnal range of AOD variation (maximum value minus minimum value of AOD in one day) for each instrument.

This can be considered as a hint pointing to the suggestion that the instrument that shows the highest daytime AOD range is the one that is responsible for the outlier, since a real symmetric AOD variability around noon of one instrument measurements, while the other shows a constant AOD during the day, is very unlikely. In most cases it is AERONET-Cimel, with a diurnal range of variation higher than 0.01 in some cases, which causes differences, as shown in Figure 3. This is attributable to an imperfect calibration that can be only be detected in extreme conditions: UV channel, very low optical air mass, and pristine conditions. According to Toledano et al. (2018), the greatest variance in the extraterrestrial constant in the UV channel could be due to a number of factors: 1) higher AOD variability at the shorter wavelengths; 2) filter blocking issues; and 3) temperature effects that affect AERONET-Cimel instruments that have not been accounted for in the UV range. One of these causes or a combination of them, could be behind the explanation of the slightly worst traceability in 380 nm in these conditions. However, it is striking to see that the number of cases in which AERONET-Cimel AOD daytime range is high, decreases drastically in the second period 2011-2015 in which practically only the Cimel #244 is used linked with lengthening the calibration periods with the Langley method, which allows a more accurate determination of the extraterrestrial constants.

Although it would be necessary to further explore this issue, it appears that most of the non-AOD traceabilities at 380 nm, under pristine conditions (AOD ≤ 0.03), are due to insufficiently accurate calibration of AERONET-Cimel in this channel.

Atmos. Meas. Tech. Discuss., https://doi.org/10.5194/amt-2018-438
Manuscript under review for journal Atmos. Meas. Tech.
Discussion started: 17 December 2018

Atmospheric Measurement Techniques Discussions

Figure 3. Diurnal range of AOD_{380nm} variation (maximum value minus minimum value of AOD in one day) corresponding to outlier (non-traceable) AOD data under pristine conditions ($AOD_{500nm} \leq 0.03$) in the period 2005-2015.

5.2.2 Differences in cloud-screening and sun tracking

In this section we examine the effect that the presence of clouds might have on AOD differences and the number of cases outside the U95 limits.

AERONET-Cimel Version 2 data uses the so-called "triplet check" cloud-screening algorithm developed by Smirnov et al. (2000) and a second-order temporal derivative constraint (McArthur et al., 2003) to rule out AOD measurements potentially contaminated by clouds. GAW-PFR algorithms also use the Smirnov triplet measurement, and the second-order derivative check, but add a test for optically thick clouds with $AOD_{500nm} > 2$ (Kazadzis et al., 2018b). This algorithm, used by both networks with certain variants, assumes a transitory character in the presence of a cloud, which causes a sudden change of AOD. This sharp change would be detected by measuring the stability of three successive optical depth measurements, so that, when a cloud totally or partially blocks the sun, the standard deviation associated with the average of the triplets increases enormously. Note that if either one or both cloud screening algorithms (GAW-PFR and AERONET-Cimel) are flagged as cloudy, then the corresponding AOD data pair does not take part in the comparison.

However, in the case of stratiform and very stable clouds or in the case of very thin clouds such as cirrus clouds, the algorithm could erroneously interpret that there are no clouds since there would be no appreciable changes in the stability of the triplets.

We do not have precise ancillary information to verify in each 1-minute data the influence that a certain cloud could cause in the non-traceability found. As a first approach for assessing the impact that cloud conditions might cause on AOD traceability, we have used the concept of daily fractions of clear sky (FCS) that has been applied before to solar radiation data at Izaña Observatory (García et al., 2014). FCS represents the percentage of observed sunshine hours in a day with respect to the maximum possible sunshine hours in that day. The higher the daily FCS, the higher the clear sky percentage we have on that day.

The percentages of traceable and non-traceable AOD data versus FCS values grouped into 5 intervals are shown in Table 7. The results indicate that with a FCS lower than 20 % (almost overcast skies), and for wavelengths lower than 870 nm, data outside the $U95$ limits comprises, at least, 50 % of the total AOD data. As the fraction of clear sky increases, the percentage of traceable AOD data significantly exceeds the number of non-traceable AOD data. The percentage of traceable data is especially large (> 90 %) when FCS > 80 % (almost clear skies). However, the real impact of clouds on AOD traceability at Izaña Observatory is very low due to its special characteristics of high mountain station with very little cloudiness. As indicated in Table 7 (figures in brackets), the percentage of cases in which FCS < 60 % is lower than 1.33 %. Therefore, in practice, the possible impact of clouds on the non-traceability of AOD data-pairs is insignificant at the Izaña Observatory since most of the time there are clear skies or skies with very little presence of clouds. On the other hand, and in order to interpret these results correctly, it should be emphasized that both GAW-PFR and AERONET-Cimel cloud screening algorithms provide successful identification on clear direct-sun conditions during cloudy skies (FCS < 40 %), 99.75 % of the cases, excluding those with very thin clouds. Future specific studies with AERONET V3 will allow to elucidate if the AOD traceability increases substantially under the presence of cirrus because its detection is one of the notable improvements of the V3 compared to V2. of AERONET V3 (Giles et al., 2018).

However, we admit that this methodology can only be used qualitatively, as it has serious limitations since sunshine recorders are not sensitive enough to detect the presence of cirrus that, to a large extent, might cause failures in cloud-screening algorithms. A more detailed analysis of more rare atmospheric conditions, such as those of strati-form and homogeneous cirrus clouds, or when altostratus are present above the Saharan Air Layer (SAL), around 6 Km altitude, and thus masked by a heavy mineral dust layer below needs further investigation. A constant cloud optical thickness (COT) corresponding to a cloud of a certain horizontal extension would cause the successive measurements within a minute to correspond to the same cloud stage, and therefore it would not be discernible from the extinction caused by aerosols. In the case of very thin cirrus clouds, the fluctuations in AOD would be very small and could be interpreted as the presence of a light layer of aerosols. Another factor that must be taken into account is that the FOV of the instruments is different. Thus, GAW-PFR (FOV = 2.5°) could detect the entry of a constant COT cloud in part of its field of view in a different way than AERONET-Cimel (FOV = 1.2°). In all these cases, the cloud-screening algorithms may fail simultaneously in both GAW-PFR and AERONET-Cimel, resulting in a different AOD measurement derived by the two instruments. These type of rare situations should be the subject of future studies through measurement campaigns using ancillary observation systems (e.g. lidar, all sky camera).

Atmos. Meas. Tech. Discuss., https://doi.org/10.5194/amt-2018-438
Manuscript under review for journal Atmos. Meas. Tech.
Discussion started: 17 December 2018

Atmospheric Measurement Techniques Discussions

Table 7. Percentage of traceable (T) data and percentage of AOD data outside the $U95$ limits (NT) for each channel and 5 FCS intervals. In brackets, relative frequency of each FCS interval.

	380 nm		440 nm		500 nm		870 nm	
	T (%)	NT (%)	T (%)	NT (%)	T (%)	NT (%)	T (%)	NT (%)
0%≤FCS<20% (0.03%)	47.6	52.4	43.5	56.5	47.6	52.4	87.0	13.0
20%≤FCS<40% (0.22%)	69.3	30.7	73.3	26.7	73.6	26.4	86.3	13.7
40%≤FCS<60% (1.08%)	79.1	20.9	87.8	12.2	88.8	11.2	91.9	8.1
60%≤FCS<80% (7.10%)	88.4	11.6	93.9	6.1	93.4	6.6	97.8	2.2
FCS≥80% (91.6%)	93.3	6.7	96.2	3.8	96.2	3.8	98.3	1.7

5.2.3 Different corrections in attenuation by Rayleigh scattering, and absorption by O_3 and NO_2

In this section we evaluate the possible 1-minute AOD data outside the $U95$ limits by the different processing that each network makes in the correction by Rayleigh scattering and by absorption of column O_3 and NO_2.

Although GAW-PFR and AERONET-Cimel use spectral channels with weak absorption by atmospheric gases, AOD can only be determined if optical depth contributions from those gases are well estimated and subtracted from the total optical depth (τ). GAW-PFR and AERONET-Cimel separate the contributions of the molecules (Rayleigh scattering, τ_R), aerosols (τ_a; in this study referred to as AOD) and absorbing gases, generally total column ozone (τ_{O3}) and nitrogen dioxide (τ_{NO2}) due to their different optical air masses at low solar elevation:

$$I(\lambda) = I_0(\lambda)\exp -(\tau_R m_R + \tau_a m_a + \tau_{O3} m_{O3} + \tau_{NO2} m_{NO2}) \quad (3)$$

So, AOD can be derived from:

$$AOD = \frac{1}{m_a}(ln\frac{I_0(\lambda)}{I(\lambda)} - \tau_R m_R - \tau_{O3} m_{O3} - \tau_{NO2} m_{NO2}) \quad (4)$$

Rayleigh scattering

The Rayleigh scattering contribution to total optical depth would be:

$$\tau_R = \delta_R \frac{m_R}{m_a} \quad (5)$$

where, m_R is written, according to Kasten and Young (1989), as:

$$m_R = \frac{1}{sin\theta + 0.50572(\theta + 6.07995)^{(-1.6364)}} \quad (6)$$

Atmos. Meas. Tech. Discuss., https://doi.org/10.5194/amt-2018-438
Manuscript under review for journal Atmos. Meas. Tech.
Discussion started: 17 December 2018

Atmospheric Measurement Techniques Discussions

and m_a, according to Kasten (1966), has the following expression:

$$m_a = \frac{1}{sin\theta + 0.0548(\theta + 2.65)^{(-1.452)}} \tag{7}$$

where θ is the sun elevation, and δ_R can be expressed as (Bodhaine et al., 1999):

$$\delta_R(\lambda) = 0.00864\lambda^{-(3.916+0.074\lambda+\frac{0.050}{\lambda})}\frac{P}{P_o} \tag{8}$$

where P_o = 1013.25 hPa, λ is the wavelength in microns (μ) and P is the pressure in hPa at the measurement site. The depolarization factor recommended by (Young, 1980) is already included in Eq. 8.

From Eq. 8, we can derive the differences in τ_R contribution ($\triangle\tau_R$):

$$\triangle\tau_R = (0.00864\lambda^{-(3.916+0.074\lambda+\frac{0.050}{\lambda})}\frac{1}{1013.25}\frac{m_R}{m_a})(P_{PFR} - P_{Cimel}) \tag{9}$$

So, the main $\triangle\tau_R$ from GAW-PFR and AERONET-Cimel might basically arise from the different way the two instruments measure the atmospheric pressure (P_{PFR} and P_{Cimel}, respectively).

While AERONET-Cimel determines the site station pressure from the National Centers for Environmental Prediction (NCEP) and the National Center for Atmospheric Research (NCAR) reanalysis at standard levels, GAW-PFR has a solid-state pressure transducer in the control box to read barometric pressure simultaneously with each PFR measurement. As Giles et al. (2018) have stated, the expected error in the station pressure P_{Cimel} is generally < 2 hPa provided the elevation of the station is well-known and the weather conditions are stable. In order to assess this possible difference, we have compared the 1-minute synchronous pressure data of both instruments, and the corresponding 1-minute $\triangle\tau_R$ from Eq. 9. Note that, in practice, this comparison is made at 6 hour intervals since the NCEP/NCAR reanalysis data are available routinely at six hourly temporal resolution (Kalnay et al., 1996). The results are depicted in Figure 4.

The results indicate that most of the1-minute pressure differences are within $\pm$ 5 hPa (Figure 4a), resulting in 1-minute $\triangle\tau_R$ data within $\pm$ 0.001. However, when pressure differences are significantly higher, as those registered at the end of 2014 (> 30 hPa) (Figure 4a), $\triangle\tau_R$ increases to significant values $\sim$ 0.01 (Figure 4b).

Taking into account that the accuracy of the new barometers built into new radiometers is about 3 hPa only dramatic barometer malfunctioning could cause $\triangle\tau_R$ > 0.01. As stated by Kazadzis et al. (2018b), the use of erroneous pressure values can lead to wavelength-dependent AOD errors and to large errors in AE. However, these flagrant barometer malfunctions are quickly detected and easily corrected if there are other pressure measurements at the station, as in our case.

Differences in O_3 absorption

The O_3 optical depth is determined with the following expression:

$$\tau_{O3}(\lambda) = \sigma_{O3}(\lambda)\frac{O_3}{1000}\frac{m_{O3}}{m_a} \tag{10}$$

Where O_3 is expressed in Dobson units (DU), and the absorption coefficients ($\sigma_{O3}(\lambda)$) take the following values (Gueymard, 1995): 0.0026 cm^{-1} (440 nm), 0.03150 cm^{-1} (500 nm), and 0.00133 cm^{-1} (870 nm). The ozone absorption is maximum in the 500 nm channel and zero in the 380 nm channel. GAW-PFR uses for m_{O3} the following expression (Komhyr, 1980):

$$m_{O3} = \frac{R+h}{\sqrt{(R+h)^2 - (R+r)^2(cos\theta)^2}} \tag{11}$$

Atmos. Meas. Tech. Discuss., https://doi.org/10.5194/amt-2018-438
Manuscript under review for journal Atmos. Meas. Tech.
Discussion started: 17 December 2018

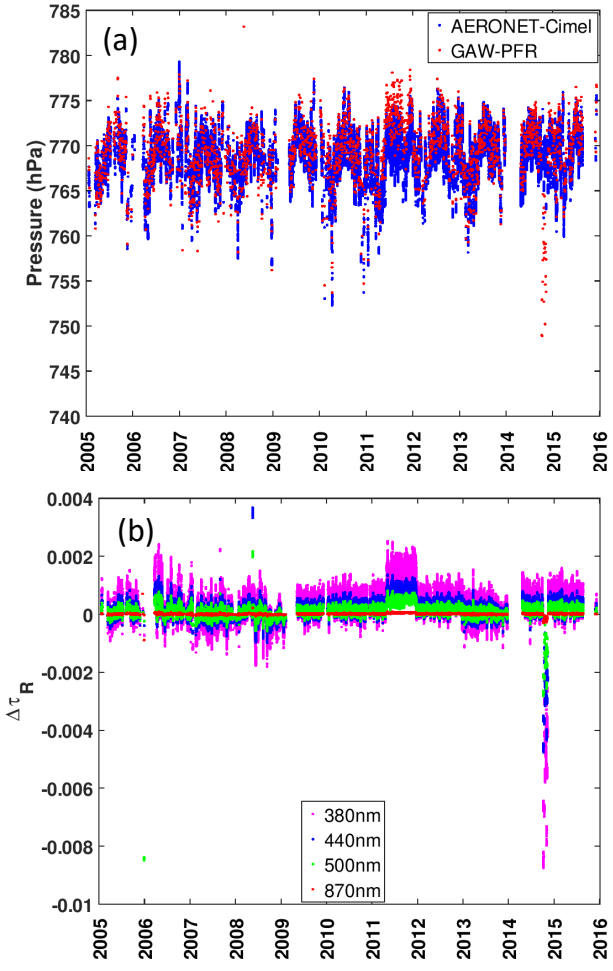

Figure 4. (a) 1-minute pressure data (hPa) from AERONET-Cimel and GAW-PFR, and (b) corresponding 1-minute $\triangle\tau_R$ caused pressure differences in the period 2005-2015.

Atmos. Meas. Tech. Discuss., https://doi.org/10.5194/amt-2018-438
Manuscript under review for journal Atmos. Meas. Tech.
Discussion started: 17 December 2018

Atmospheric Measurement Techniques Discussions

where R = 6370 km is the mean radius of the Earth, r = 2.370 km is the altitude of the station, h = 22 km is the estimated height of the ozone layer, and θ is the solar elevation. However, AERONET-Cimel uses an updated expression (Komhyr et al., 1989) in which h is not fixed and takes a value in function of the latitude and the absorption coefficients are obtained for each particular filter using the spectral response provided by the manufacturer.

For most of the period covered in this study, measured total ozone values from the GAW Izaña station were used to calculate τ_{O3} (Wehrli, 2008a). If no Brewer data is available, data retrieved from the Total Ozone Mapping Spectrometer (TOMS) satellite-sensor was used. Nowadays, GAW-PFR uses ozone data from AURA satellite overpass observations with the Ozone Monitoring Instrument (OMI) (McPeters et al., 2015) for daily operations (Kazadzis et al., 2018b). Concerning AERONET-Cimel Version 2, a NASA TOMS 1°x1.25° resolution O_3 climatology is used.

From Eq. 10, the differences in O_3 optical depth $\triangle\tau_{O3}$ can be derived:

$$\triangle\tau_{O3} = \sigma_{O3}(\lambda)\frac{1}{1000}\frac{m_{O3}(O_{3PFR} - O_{3Cimel})}{m_a} \tag{12}$$

The largest influence of total ozone data uncertainty in τ_{O3} occurs, by far, at 500 nm (Figure 5). According to Wehrli (2008b) and Kazadzis et al. (2018b), total ozone needs to be determined to $\pm$ 30 DU or 10 % of typical values, to ensure an uncertainty of $\pm$ 0.001 τ_{O3} at 500 nm. In the case of the GAW-PFR / AERONET-Cimel comparison, and due to the very different method in which both networks obtained O_3 values for their corresponding corrections, the ozone differences found on some days (1761 out of 71965 days; 2.4 %) are very large (> 40 DU), exceeding a difference in the ozone optical depth of 0.001. Even so, the potential contribution of AOD differences outside the $U95$ limits between the two networks is negligible. Total O_3 over the Izaña Observatory is quite stable, showing a relatively small amplitude throughout the year. However, if we wanted to repeat this traceability study of 1-minute AOD data in mid or high latitude stations where sharp O_3 variations (several tens of DU) could be registered in a few hours, the correction of 1-minute AOD measurements by τ_{O3} might be a challenging issue.

Differences in NO_2 absorption

AERONET-Cimel applies a correction by absorption of NO_2, but GAW-PFR does not include this correction. AERONET-Cimel obtains daily total NO_2 data from a 0.25°x0.2° resolution NO_2 monthly climatology obtained from the ESA SCanning Imaging Absorption SpectroMeter for Atmospheric CHartographY (SCIAMACHY) (Eskes and Boersma, 2003). In order to assess the contribution in AERONET-Cimel 1-minute AOD data non-traceability by NO_2 absorption what we really estimate is the NO_2 optical depth ($\tau_{NO2}(\lambda)$) of AERONET-Cimel since GAW-PFR does not perform this correction. Analogously to $\triangle\tau_{O3}$, the differences in nitrogen dioxide optical depth $\triangle\tau_{NO2}$ can be obtained from:

$$\triangle\tau_{NO2} = \sigma_{NO2}(\lambda)\frac{1}{1000}\frac{m_{NO2}}{m_a}(-NO_{2Cimel}) \tag{13}$$

Where m_a is given by Eq. 7, NO_{2Cimel} (DU) is the daily total NO_2 used by AERONET-Cimel, $\sigma_{NO2}(\lambda)$ is the NO_2 absorption coefficient with values that depend on wavelength (Gueymard, 1995) and are weighted by the specific filter response: 15.6 cm^{-1} (380 nm), 12.3 cm^{-1} (440 nm), and 4.62 cm^{-1} (500 nm), and m_{NO2} has the following expression (Gueymard, 1995):

$$m_{NO2} = \frac{1}{sin\theta + 602.30(90-\theta)^{0.5}(27.96+\theta)^{-3.4536}} \tag{14}$$

Atmos. Meas. Tech. Discuss., https://doi.org/10.5194/amt-2018-438
Manuscript under review for journal Atmos. Meas. Tech.
Discussion started: 17 December 2018

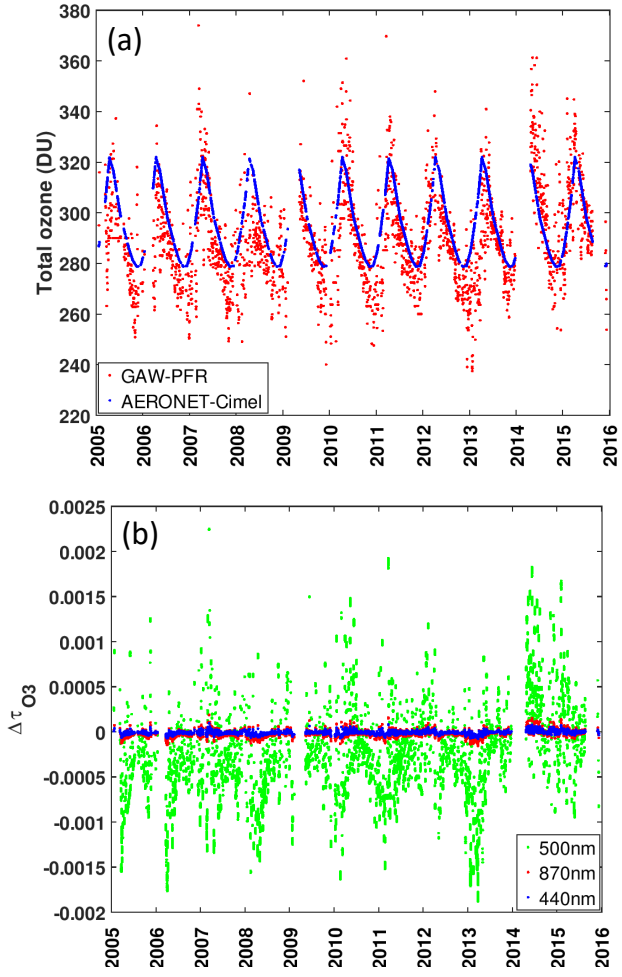

Figure 5. (a) Total O_3 used by GAW-PFR and AERONET-Cimel, and (b) $\triangle\tau_{O3}$ (λ) caused by differences in daily total O_3 between the two instruments in the period 2005-2015.

Atmos. Meas. Tech. Discuss., https://doi.org/10.5194/amt-2018-438
Manuscript under review for journal Atmos. Meas. Tech.
Discussion started: 17 December 2018

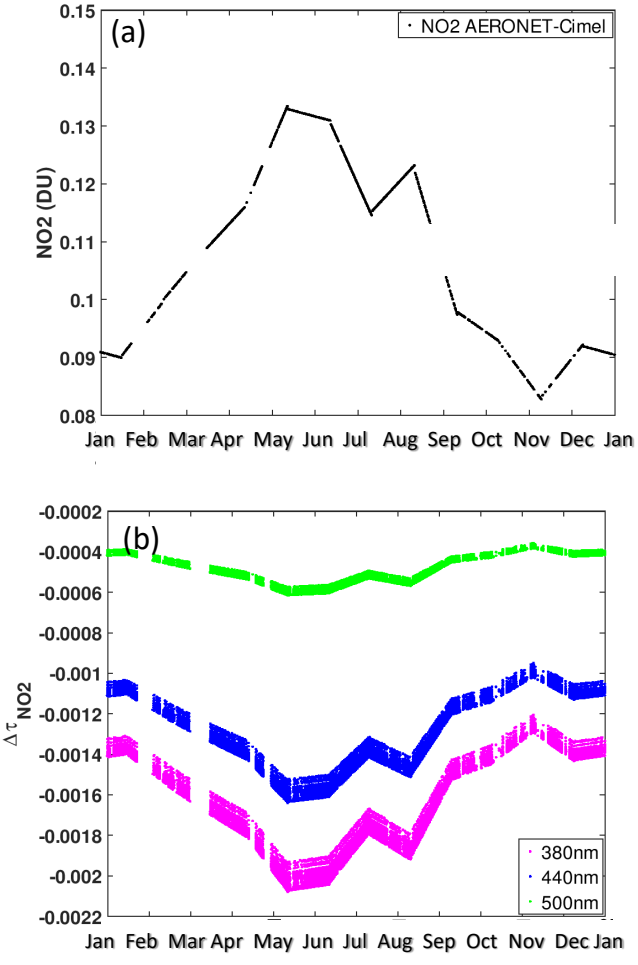

Figure 6. (a) NO_2 annual course from a NO_2 monthly climatology obtained from the ESA SCanning Imaging Absorption SpectroMeter for Atmospheric CHartographY (SCIAMACHY), used by AERONET-Cimel at Izaña Observatory, and (b) $\triangle\sigma_{NO2}$ (λ) caused by differences in daily total NO_2 between GAW-PFR and AERONET-Cimel in the period 2005-2015. Note that GAW-PFR does not take into account the correction for the NO_2 absorption.

Atmos. Meas. Tech. Discuss., https://doi.org/10.5194/amt-2018-438
Manuscript under review for journal Atmos. Meas. Tech.
Discussion started: 17 December 2018

Atmospheric Measurement Techniques Discussions

Table 8. Percentage (%) of traceable AERONET-Cimel AOD 1-minute data and AOD data outside the $U95$ limits that become traceable after correcting by pressure, and total column O_3 and NO_2.

Channel	Traceable AERONET-Cimel data (%)	Increment (%) of traceable data after P, O_3 and NO_2 corrections
380 nm	92.7	1.3
440 nm	95.7	0.2
500 nm	95.8	0.3
870 nm	98.0	$\sim$ 0.0

In Figure 6a the total NO_2 used by AERONET-Cimel to evaluate $\tau_{NO2}(\lambda)$ is depicted. Figure 6b shows the $\triangle\sigma_{NO2}(\lambda)$ caused by differences in daily total NO_2 between GAW-PFR and AERONET-Cimel. $\triangle\sigma_{NO2}$ is of the order of 10^{-3} for 380 and 440 nm channels, while, for 500 nm channel, it is of the order of 10^{-4}. As for O_3, the absorption due to total NO_2 is negligible in the 1-minute AOD non-traceability in our study. However, it must be taken into account if this type of traceability analysis is replicated in highly polluted regions where the NO_2 absorption might have some impact on AOD, such as in large industrial cities, in which tropospheric NO_2 adds to the natural stratospheric NO_2 resulting in column values much larger than the climatological ones (Chubarova et al., 2016).

Taking into account the corrections for Rayleigh scattering and for the absorptions by O_3 and NO_2, we have calculated the combined effect of all of them on the non-traceability of the 1-minute AOD values (Figure 6; Table 8). At most (in the 380 nm channel), 25 % (1.3 % of total common measurements) of data outside the $U95$ limits are due to significant differences in pressure, and in O_3 and NO_2 absorption. Most of the AOD data outside the $U95$ limits that becomes traceable data after corrections are applied, had errors in the pressure measurement and therefore in the Rayleigh scattering correction. The 1-minute AOD data outside the $U95$ limits by these corrections is negligible in the 870 nm channel.

5.3 GAW PFR and AERONET-Cimel comparison under high AOD conditions: the role of the different FOV

When we represent the AOD differences between AERONET-Cimel and GAW-PFR versus AOD (GAW-PFR) we observe a positive slope that increases when the AOD fitted data are > 0.05 (non-pristine conditions), noting that AERONET-Cimel shows higher AOD values than GAW-PFR, being higher than +0.01 for AOD > 0.15 (Figure 7), and more clearly at 500 nm. The AOD data outside the $U95$ limits (in red) increases notably from AOD > 0.1.

In fact, the percentage of non-traceable AOD data increases as AOD increases (Table 9), so that for dust related aerosol conditions (AOD_{500nm} > 0.3) the percentage of AOD data outside the $U95$ limits is > 50 % for all channels except for 870 nm (Table 9, percentages in brackets). The increase in the percentage of AOD data outside the $U95$ limits is especially significant at the 380 nm channel.

These results show a non-negligible percentage of AOD differences outside the $U95$ limits for AOD > 0.1, ranging from $\sim$ 0.3 % at 870 nm to $\sim$ 1.9 % at 380 nm. This especially affects the shorter wavelengths (Table 9).

Atmos. Meas. Tech. Discuss., https://doi.org/10.5194/amt-2018-438
Manuscript under review for journal Atmos. Meas. Tech.
Discussion started: 17 December 2018

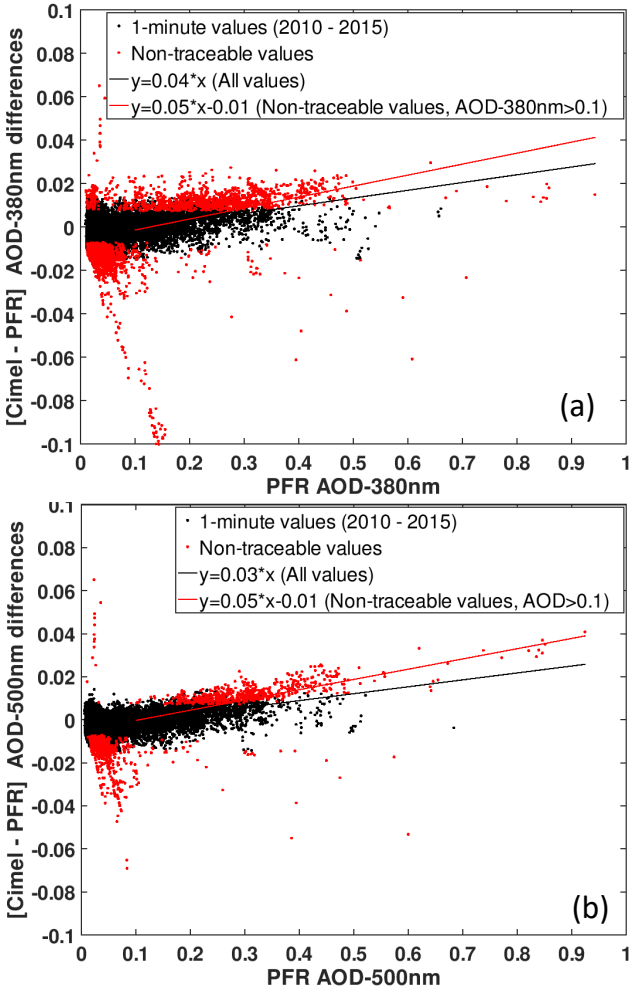

Figure 7. Actual AOD differences between AERONET-Cimel and GAW-PFR vs PFR AOD at (a) 380 nm (b) and 500 nm for the period 2010-2015.

Table 9. Percentage of AOD data outside the $U95$ limits at 380, 440, 500 and 870 nm channels and for three AOD_{500nm} thresholds respect to all data and respect to all data for each AOD interval (in brackets).

	Percentage of AOD data outside the $U95$ limits (%)		
	AOD_{500nm}>0.1	AOD_{500nm}>0.2	AOD_{500nm}>0.3
380 nm	1.9 (25.0)	1.2 (47.2)	0.5 (59.8)
440 nm	1.0 (13.5)	0.8 (32.0)	0.5 (57.6)
500 nm	1.1 (14.9)	0.9 (35.1)	0.5 (60.8)
870 nm	0.3 (4.1)	0.2 (6.4)	0.1 (14.0)

Atmos. Meas. Tech. Discuss., https://doi.org/10.5194/amt-2018-438
Manuscript under review for journal Atmos. Meas. Tech.
Discussion started: 17 December 2018

Torres et al. (2013) investigated the uncertainty of the FOV in the AERONET-Cimel measurements indicating that direct solar irradiance measurements are biased by the amount of aureole radiation that is assumed to be direct solar radiation. The solar aureole, also known as the circumsolar region, is the bright region surrounding the solar disc, which becomes especially visible when there is a burden of moderate-high aerosols in the atmosphere. GAW-PFR has double the FOV (2.5°; Wehrli (2000)) compared to the AERONET-Cimel (1.2° ± 10 %; Torres et al. (2013)), so it is reasonable to expect that it is more affected by the circumsolar radiation than the AERONET-Cimel radiometer.

In this section we make a first analysis on the role that the FOV might play to explain the AOD differences between GAW-PFR and AERONET-Cimel for relatively high dust load (AOD > 0.1) conditions. To do this we used a simplistic approach using the SMARTS model to determine the circumsolar radiation and the direct irradiance of each radiometer with different FOV.

The estimated value of the circumsolar irradiance within the radiometer has been calculated with the SMARTS model version 2.9.5 (Gueymard, 1995). We have used a configuration that includes a subtropical summer atmosphere, a desert aerosol mode (DESERTMAX), and an average surface albedo of 0.11. This configuration is the best suited to the conditions of SAL intrusions with high mineral dust content. As input data SMARTS uses the coordinates of the site, date and time, pressure, total column O_3, and AOD_{500nm}. The extraterrestrial spectrum is the new Kurucz spectrum (Chance and Kurucz, 2010). For the PFR, a slope angle of 0.72°; opening half-angle of 1.25°, and limit angle of 1.79° were measured and used as input view geometry parameters in the SMARTS model following Blanc et al. (2014). In the case of AERONET-Cimel, the FOV (0.6445° ± 0.025°) coincides with the opening half-angle, and can be theoretically calculated using the focal length of the first lens (100 mm) and the radius of the FOV defining aperture (1.125 mm) according to Wilbert (2014).

The ratio of circumsolar radiation to direct radiation from GAW-PFR at 380 and 500 nm has been plotted against that of the AERONET-Cimel using their respective FOV and AOD data (Figure 8a and 8b; black dots). The GAW-PFR circumsolar radiation is ∼ 2.7 and 2.9 times higher than that of AERONET-Cimel at 380 nm and 500 nm, respectively for the same atmospheric conditions (Figure 8a and 8b). The great dispersion of data is due to the fact that they correspond to different optical air mass values.

The slope of the linear regression is 0.51 and 0.60 at 380 nm and 500 nm, respectively. When this ratio is calculated using the PFR AOD but modifying the FOV to 1.2° and the FWHM to 10 nm, in order to simulate the AERONET-Cimel, a quite similar result is obtained (Figure 8c and 8d; blue dots) with a slope of the linear regression of 0.52 for 380 nm and 0.61 for 500 nm, confirming that the difference in FOV between GAW-PFR and AERONET-Cimel modulates the differences in circumsolar radiation. We have found that this relationship depends on the optical air mass, obtaining higher slopes for low optical air mass. There is a clear relationship between the PFR AOD and the ratio of circumsolar radiation to direct radiation from AERONET-Cimel and from GAW-PFR (Figure 8c and 8d). The major differences in AOD between GAW-PFR and AERONET-Cimel, due to the different circumsolar radiation, are recorded for optical air mass < 3. For example, at 500 nm, a GAW-PFR ratio of circumsolar radiation to direct radiation equal to 2 (0.71 for AERONET-Cimel) results in an AOD difference between AERONET-Cimel and GAW-PFR of ∼ 0.02, and ∼ 0.01 between GAW-PFR with reduced FOV and GAW-PFR. These results

Atmos. Meas. Tech. Discuss., https://doi.org/10.5194/amt-2018-438
Manuscript under review for journal Atmos. Meas. Tech.
Discussion started: 17 December 2018

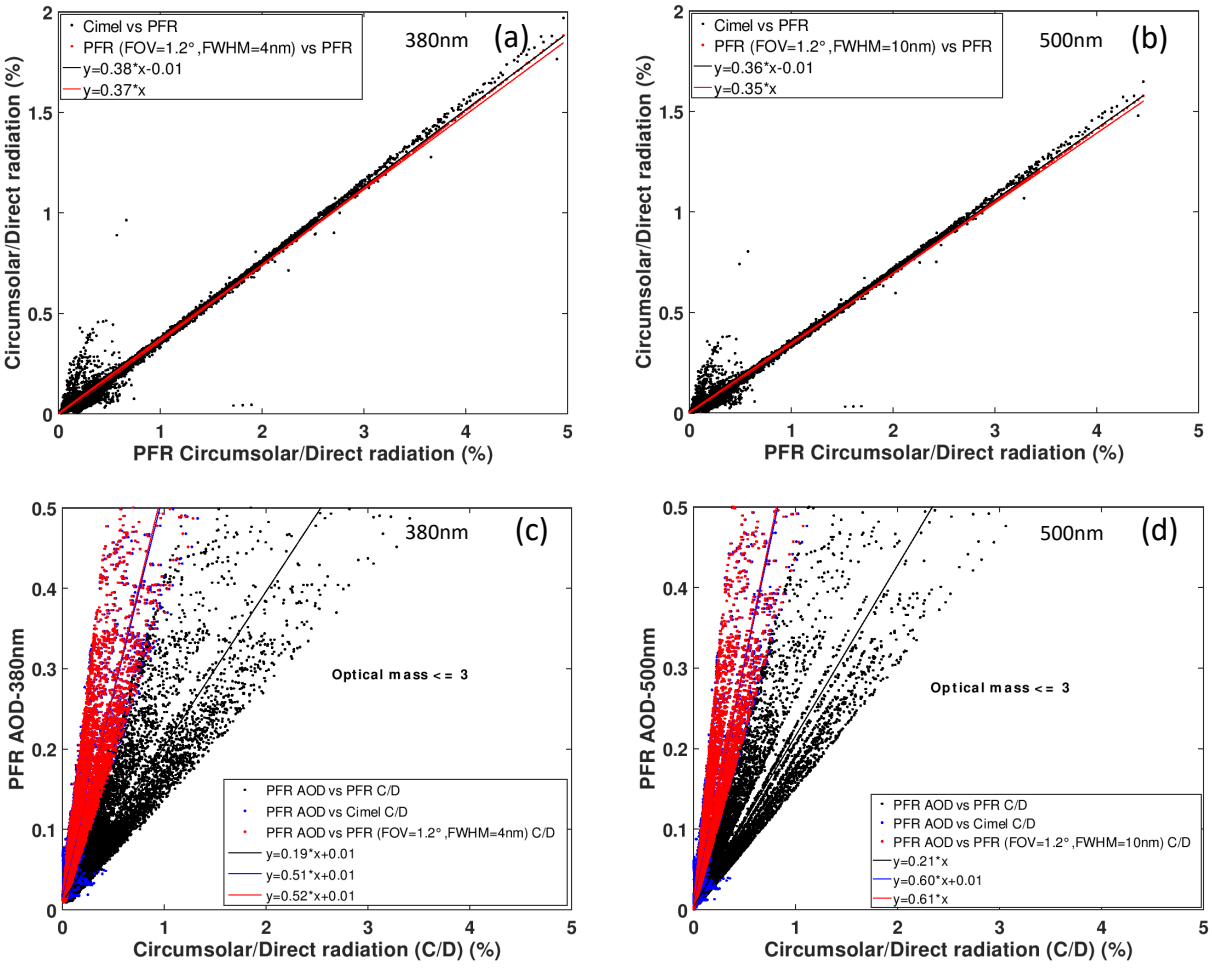

Figure 8. Ratio of circumsolar radiation to direct radiation from AERONET-Cimel and from GAW-PFR using the Cimel FOV and FWHM vs ratio of circumsolar radiation to direct radiation from GAW-PFR at (a) 380 nm and (b) 500 nm. GAW-PFR AOD vs ratio of circumsolar radiation to direct radiation at (c) 380 nm and (d) 500 nm for the period 2005-2015.

Atmos. Meas. Tech. Discuss., https://doi.org/10.5194/amt-2018-438
Manuscript under review for journal Atmos. Meas. Tech.
Discussion started: 17 December 2018

are consistent with some AOD differences found for $AOD_{500nm} > 0.1$ that cause non-traceability, but this analysis should be only considered as a first approximation to the correction of AOD by FOV.

Summarizing, these preliminary results indicate that a non-negligible percentage of non-traceable 1-minute AOD data under dusty conditions (AOD > 0.1) might be explained, at least partially, by the different FOV of the two radiometers. However, a detailed study on the impact might cause a different FOV in the AOD retrieval, and a corresponding uncertainty analysis (Eissa et al., 2018), must be performed. This is not a trivial task since a simulation using a more complex radiative transfer model that includes accurate dust aerosol forward scattering effects as formulated by Ge et al. (2011) would be needed. Furthermore, it should be taken into account that, as discussed in section 5.2.2., under relatively high AOD conditions, the presence of altostratus above SAL is not infrequent, and they could also cause non-traceability in AOD when the cloud screening algorithms fail. Therefore, the FOV study should be done once the dust events with presence of clouds over the SAL have been ruled out.

The effect of FOV on AOD retrieval should be taken into account for those radiometers with a relatively high FOV measuring in regions with relatively high AOD (> 0.2) for most of the year (Basart et al., 2009; Cuevas et al., 2015; Eck et al., 1999; Kim et al., 2007), as is the case in many places of Northern Africa, the Middle East and East Asia. This effect could lead to AOD underestimation, and the variable number of high AOD episodes in each season of the year might affect the AOD long-term trends. AOD measurements under these conditions would be especially affected for optical air mass < 3.

5.4 Angström exponent comparison

We have performed a comparison of the AE provided by GAW-PFR and AERONET-Cimel using in both cases the AOD data obtained from the four common channels with a total of 70716 data-pairs. AE differences > 0.2 increase exponentially for AOD < 0.02, reaching AE differences of up to 1.6 under pristine conditions (Figure 9a). For very low AOD the provided instruments uncertainty is the source of the sharp increase in AE, and at the same time AE becomes very sensitive to slight AOD changes. However, for AOD < 0.02 the atmospheric aerosol load is practically zero and so, its characterization with AE have relatively minor importance, in practice.

In addition, the AE differences remain below 0.1 when AE_{PFR} values are below 1 (Figure 9b), which shows that these differences are small in most of the possible atmospheric scenarios. For $1 < AE_{PFR} < 1.2$ the AE differences increase slightly to values below 0.2, and for $AE_{PFR} > 1.2$ (very fine particles or pristine conditions) the AE differences increase sharply to reach values around 1.2. In our case, the non-pristine conditions or those with a high content of mineral dust have associated AOD > 0.03 and AE < 1, where the AE differences remain below 0.1. In case of pristine conditions AOD $\leq$ 0.03 and AE $\geq$ 1 the AE differences can reach a maximum of 1.6.

Wagner and Silva (2008) estimated the usual maximum AE error by error propagation using a pair of spectral channels in which AOD is measured. Their results show that for clean optical conditions (AOD_{440nm}= 0.06) the maximum AE error is 1.17, and for hazy conditions (AOD_{440nm}=0.17) the error is 0.17, assuming an underlying AE of 1.5. These values drop down to 0.73 and 0.11, respectively, if AE=0. The AE differences found between GAW-PFR and AERONET-Cimel lie within the estimated errors reported by Wagner and Silva (2008).

Atmos. Meas. Tech. Discuss., https://doi.org/10.5194/amt-2018-438
Manuscript under review for journal Atmos. Meas. Tech.
Discussion started: 17 December 2018

Table 10. Uncertainty in AE determination for three typical atmospheric situations.

	Uncertainty in AE
Normal pristine conditions AOD_{500nm}= 0.03 and AE = 1.4	≥ 1
Hazy conditions AOD_{500nm}= 0.14 and AE = 1.15	≥ 0.2
Strong dust intrusion AOD_{500nm}= 0.3 and AE = 0.3	~ 0

In any case, as in our study the AE has been determined from AOD measured in the four common channels of GAW-PFR and AERONET-Cimel, we have made an estimate of the uncertainty in the calculation of the AE for three scenarios that are typically recorded at Izaña. These estimations have been calculated following the Wagner and Silva (2008) methodology but including the AOD uncertainty related with each of the two instruments and for different conditions. The uncertainty estimations are shown in Table 10. The AE derived from more than 2 wavelengths is less affected by AOD inaccuracies than AE calculated with pairs of wavelengths, since the latter are calculated from the ratio of AOD at two channels (Cachorro et al., 2008).

The AE differences of our study (Figure 9) are within the AE uncertainty estimated for each type of atmospheric condition (pristine, hazy and heavily dust loaded).

However, although AE is a quantitative parameter, it is only used in a qualitative way to estimate the range of sizes (fine, medium, coarse) of the predominant aerosol in the inevitable mixture of aerosols that we observe. With this parameter, and together with the information that is available in the measurement site about the most frequent types of aerosols and their concentration, we can estimate the type of aerosols that are being measured.

There are many publications with different thresholds of AE and AOD in order to classify different types of aerosols (e.g. Basart et al., 2009; Cuevas et al., 2015; Dubovik et al., 2002; Guirado et al., 2014; Holben et al., 2001; Kim et al., 2007; Todd et al., 2007; Toledano et al., 2007; Wang et al., 2004). However, there is no consensus on these thresholds since at each site there are different mixtures of aerosols, and each type of aerosol shows specific frequencies of appearance and different concentrations.

Taking into account all of the above, an alternative way of analyzing the degree of agreement in AE between GAW-PFR and AERONET-Cimel is to verify to what extent both networks provide the same information regarding the type of aerosol they observe.

As an example, and according to the studies referenced above, we have established the following three main classes of aerosol scenarios present in most of the situations at the Izaña Observatory based on the AE value:

1. AE > 0.7: Pristine conditions.
2. 0.3 < AE_{PFR} & $AE_{Cimel} \leq 0.7$: Hazy, being mineral dust the main aerosol component.
3. AE $\leq$ 0.3: Pure dust.

Atmos. Meas. Tech. Discuss., https://doi.org/10.5194/amt-2018-438
Manuscript under review for journal Atmos. Meas. Tech.
Discussion started: 17 December 2018

Atmospheric Measurement Techniques Discussions

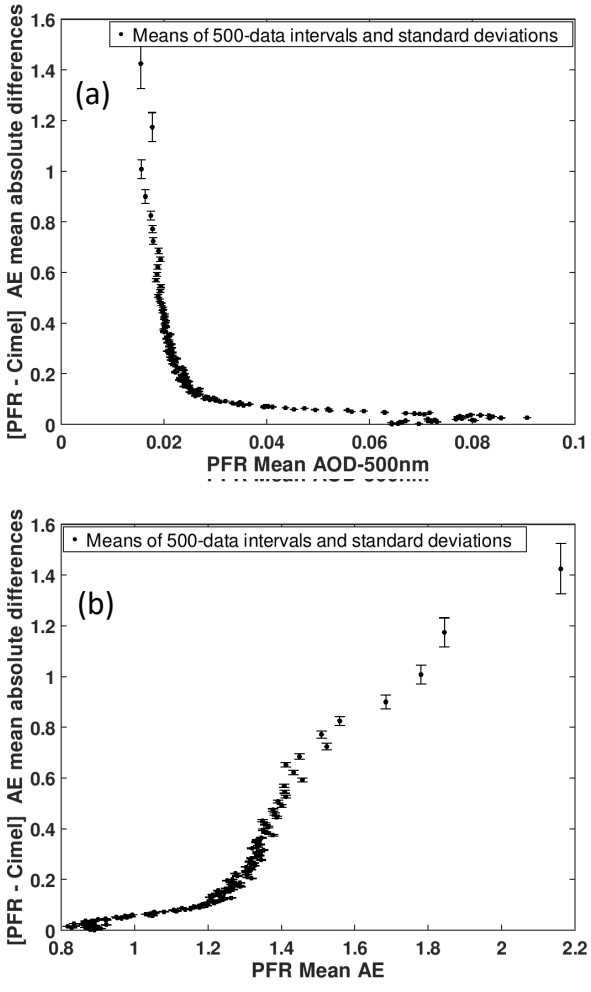

Figure 9. (a) PFR-Cimel AE mean absolute differences vs PFR mean AOD_{500nm} in 500 data intervals (b) and vs PFR mean AE in 500 data intervals.

In 93.8 % of the cases GAW-PFR and AERONET-Cimel match the AE intervals of each aerosol scenario. Most of the agreement (79 %) occurs in the predominant scenario of pristine conditions despite the AE uncertainty under pristine conditions being ≥ 1. Notice that given the special characteristics of the Izaña Observatory, AE is a self-sufficient parameter to define different types of aerosol scenarios without the need to combine its information with AOD.

6 Summary and Conclusions

In this study, a long-term comparison of synchronous 1-minute AOD data from GAW-PFR and AERONET-Cimel was carried out in four wavelengths (380, 440, 500 and 870 nm) for an 11 year period (2005-2015).

While GAW-PFR is the AOD reference globally, being directly linked to WMO / CIMO, and was specifically designed to detect long-term AOD trends, AERONET-Cimel is the densest AOD measurement network globally, and the network most frequently used for aerosol characterization and for model and satellite observation evaluation. However, these networks use radiometers that have important technical differences, and very different calibration and evaluation methodologies, and their calibration systems are completely independent of one another. Moreover, the AERONET-Cimel 11-year AOD data series at Izaña Observatory was obtained using a large number of radiometers. A total of 13 reference instruments (Masters) in the period 2005-2009, which means that every 4 and a half months, approximately, an instrument was replaced by another one to be calibrated. Their calibrations were performed during their respective measurement time periods at Izaña Observatory. Therefore, these calibrations were not in any way linked with those of the instruments that preceded or replaced them, nor with GAW-PFR reference. This fact introduced some concern about the homogeneity of the AERONET-Cimel AOD data series and their intercomparability with the much more homogeneous AOD data series from GAW-PFR.

The objective of this study is to assess whether, despite the marked differences between both networks, and the different day to day maintenance and operation procedures of the respective instruments during the study period, it is possible to consider that the information provided in the long term by the two networks is comparable and consistent. The traceability concept for AOD suggested by WMO consists in determining whether the AOD difference of the AERONET CIMELs vs the GAW PFRs lie within specific limits.

We have used uncertainty limits for AOD traceability established by WMO (2005) for this type of instruments with finite FOV. The acceptable traceability is when 95 % of the absolute AOD differences lie within these limits, in which case both data populations are considered equivalent. It should be clarified that “traceability” is not used in a strict metrological sense.

More than 70000 synchronous GAW-PFR (PFR) and AERONET-Cimel (Cimel) 1- minute data-pairs in each channel in the period 2005-2015 were analysed. An excellent traceability of AOD from the AERONET-Cimel is found in the four channels. The lowest percentage of traceable AOD data is registered in 380 nm with 92.7 % of the 1-minute data within the WMO limits, and the highest in 870 nm with 98.0 % of the data. The percentage of traceable data-pairs

The 1-minute AOD-differences Mean Bias of this study is 0.001, an order of magnitude lower than those obtained from previous short-term PFR-Cimel comparison campaigns, in which the Cimel instruments were calibrated by transferring the

calibration coefficients by comparison with co-located Master instruments. This indicates the importance of good calibration and maintenance of the Cimel instruments to obtain AOD data very similar to that of GAW-PFR.

In this study, since the AERONET-Cimel radiometers were calibrated using the Langley plot technique at the Izaña Observatory, and the calibrations of the GAW-PFRs are directly traceable to the WMO-GAW reference, being double-checked by Langley plot calibrations at Izaña, we have the best possible calibrations in the instruments used by both networks.

The results confirm that the AOD data outside the $U95$ limits due to calibration related errors is quite small and not observable for 440, 500 and 870 nm since AOD non-traceability is < 2.1 % for pristine conditions ($AOD_{500nm} \leq 0.03$) in these channels. In addition, no dependence of the 1-minute AOD differences with the air optical mass is observed. However, for 380 nm the percentage of non-traceable values increases up to 5.5 % for $1 \leq$ m < 2, being the most likely cause an insufficient accurate calibration of AERONET-Cimel in this channel.

Small misalignments in the sun-pointing constitute a serious problem and a major cause of non-traceability of AOD data-pairs as demonstrated by the AOD data outside the $U95$ limits from the period 2005-2010 as a consequence of episodic problems with the sun-tracker of the GAW-PFR radiometer. For the 2010-2015 period the percentage of traceable data-pairs improves to 93.5% (380 nm), 97.4% (440 nm), 97.2% (500 nm) and 99.1% (870 nm).

Regarding AOD non-traceability due to the different cloud-screening algorithms of both networks, it must be said that both algorithms are very similar. GAW-PFR uses the same cloud screening as AERONET-Cimel but incorporates some additional controls. The only reason for AOD non-traceability comes from the simultaneous failure of both cloud screening algorithms because if one or both of them detect clouds, the data will not be part of the comparison. According to our observations, the simultaneous failure of both cloud screening algorithms might occur only under the presence of large and stable cirrus, or altostratus ($\sim$ 6000 m a.s.l.) on the top of a heavily dust loaded Saharan air layer, hiding very wide and stable clouds. In these cases the radiometers interpret these clouds as aerosols and might provide very different values of what is really cloud optical depth.

According to our analysis, only dramatic barometer malfunctioning of one of the instruments could cause significant differences in the Rayleigh scattering contribution to total optical depth, and hence AOD non-traceability. Since the accuracy of the new barometers built into new radiometers is about 3 hPa, and only errors in atmospheric pressure > 30 hPa might produce an impact on Rayleigh scattering, the AOD non-traceability due to errors in Rayleigh scattering is negligible. The impact of barometer malfunctioning is well detected because it leads to wavelength-dependent AOD errors and to large errors in Ångström exponent.

The largest influence of total ozone data uncertainty in ozone absorption occurs mainly at 500 nm. Total ozone needs to be determined to $\pm$30 DU or 10 % of typical values, to ensure an uncertainty of $\pm$0.001 ozone absorption at 500 nm. In the case of the GAW-PFR / AERONET-Cimel comparison, despite the very different methods in which both networks obtained O_3 values for their corresponding corrections, large ozone differences were found (> 40 DU) only on 2.4 % of the days (1761 out of 71965 data), resulting in a difference in the ozone optical depth slightly above $\sim$0.001. Even so, the potential contribution to non-traceable AOD values between the two networks is negligible. However, in mid or high latitude stations where fast O_3

variations of several tens of DU might be registered, the correction of 1-minute AOD measurements by ozone absorption might be an issue to be considered.

The differences in NO_2 absorption caused by differences in daily total NO_2 between GAW-PFR and AERONET-Cimel is of the order of 10^{-3} for 380 nm and 440 nm channels, while, for 500 nm channel, it is even lower, of the order of 10^{-4}. So, differences in NO_2 absorption are negligible in the 1-minute AOD non-traceability of our study. However, NO_2 absorption might have some impact in AOD in highly polluted regions, such as in large industrial cities, where column NO_2 values are much larger than the climatological ones.

Taking into account the corrections for Rayleigh scattering and for the absorptions by O_3 and NO_2, we have calculated the combined effect of all of them on the non-traceability of the 1-minute AOD values. The highest impact occurs in the 380nm channel, in which 25 % of the AOD data outside the $U95$ limits are due to significant differences in pressure, and in O_3 and NO_2 absorption. Most of the AOD data outside the $U95$ limits that becomes traceable data after corrections are applied had errors in the pressure measurement and therefore in the Rayleigh scattering correction. The 1-minute AOD data outside the $U95$ limits by these corrections is negligible in the 870 nm channel. This suggests that, probably, CIMO traceability limits shouted redefined as a function of wavelength.

We have to note that the excellent results of this 11 year comparison and the small differences found under the strict $U95$ criterion cannot be linked with the relatively low AODs that can be found at IZO. This is because absolute calibration errors contribute to the AOD calculation in an absolute way so larger than 1 % calibration errors for a given period of time can lead to even negative AOD calculations for IZO site.

The AOD differences between AERONET-Cimel and GAW-PFR versus AOD (GAW-PFR) show a positive slope that increases when the AOD fitted data are > 0.05. Therefore, as AOD increases the AOD differences increase, noting that AERONET-Cimel shows AOD values higher than GAW-PFR. Since GAW-PFR has double the FOV ($\sim$2.5°) compared to the AERONET-Cimel ($\sim$1.2°), and direct solar irradiance measurements are biased by the amount of aureole radiation that is assumed to be direct solar radiation, it is reasonable to expect that GAW-PFR is more affected by the circumsolar irradiance than AERONET-Cimel radiometer when AOD is relatively high. However, we have to bear in mind that WMO defines the PFR FOV as the recommended one for sun radiometers. We have explained part of the non-traceabilities found for relatively high AOD values, by analysing the relationship between the differences in circumsolar radiation measured by both instruments with the differences observed in AOD. We have observed a clear relationship between the Cimel-PFR AOD differences and the PFR-Cimel circumsolar radiation differences, with the slope of the fitted line greater for shorter wavelengths (380 nm). These results show that a non-negligible percentage of the non-traceable 1-minute AOD data for AOD > 0.1, ranging from $\sim$0.3 % at 870 nm to $\sim$1.9 % at 380 nm, might be caused by the different FOV. This systematic error especially affects the shorter wavelengths. This error can be especially important in dusty regions if radiometers with relatively large FOV are used.

A comparison of the AE provided by GAW-PFR and AERONET-Cimel has been performed using in both cases AOD data obtained from the four nearby common channels with a total of 70716 data-pairs. This is a very strict AE calculation since it is necessary that AOD be accurately measured by the four channels simultaneously. AE differences > 0.2 increase exponentially under very pristine conditions (AOD $\leq$ 0.03 and AE $\geq$ 1), reaching AE differences of up to 1.6. However,

for these conditions the atmospheric aerosol load is practically zero and so, its characterization with AE does not have any importance in practice. Under non-pristine conditions or those with a high mineral dust content (associated AOD > 0.03 and AE < 1), the AE differences remain below 0.1.

Summarizing, we have presented for the first time a long term comparison among different types of radiometers belonging to different aerosol global networks. From this comprehensive comparison analysis of the 1-minute AOD and AE data provided by the GAW-PFR and AERONET-Cimel instruments operating at the Izaña Observatory in the 2005-2015 period, we can conclude that the biases in the statistics are very small (< 0.003 in all channels) and therefore both are representative of the same AOD population. It should be noted that AOD traceability at 380 nm (92.7 %) does not reach 95 % of the common data, the percentage recommended by WMO $U95$ criterion, so more efforts should be made to improve AOD in the UV range.

The widely deployed AERONET-Cimel and GAW-PFR play a crucial role in understanding AOD long-term changes and detecting trends, so it would be desirable for both networks to be linked to the same GAW-WMO related reference. In this sense, these results will be used in future studies, not only to evaluate long term AOD trends at Izaña Observatory based on two independent instruments, but also to provide additional insight on long-term AOD trend analysis, and its significance and validity, based on single instruments and their calibration and AOD processing procedure and uncertainty budget. Finally, special attention should be paid to the AERONET-Cimel AOD data series used in trend detection in combination with the used data set homogeneity and their periodic calibration transfer from Master instruments.

Competing interests. The authors declare that they have no conflict of interest.

Acknowledgements. The authors thank Luc Blarel and Philippe Goloub (LOA, CNRS-University of Lille, France) for supervising the periodic calibrations of the Cimel Masters. This study has been performed in the frame of the WMO CIMO Izaña Testbed for Aerosols and Water Vapour Remote Sensing Instruments. The work was supported by the project "The Global Atmosphere Watch Precision Filter Radiometer (GAW-PFR) Network for Aerosol Optical Depth long term measurements" supported by Bundesamt für Meteorologie und Klimatologie MeteoSchweiz – GCOS Swiss Office. Part of the AERONET-Cimel radiometers have been calibrated at Izaña Observatory by AERONET-EUROPE Calibration Service, financed by the European Community specific programs for Integrating Activities: Research Infrastructure Action under the Seventh Framework Programme (FP7/2007-2013), ACTRIS grant agreement No. 262254, and Horizon 2020 Research and Innovation Program, ACTRIS-2 grant agreement No. 654109. This research has received funding from the European Union's Horizon 2020 Research and Innovation Programme under grant agreement No. 654109 (ACTRIS-2).The funding by MINECO (CTM2015-66742-R) and Junta de Castilla y León (VA100P17) is also gratefully acknowledged. We thank the staff of the Izaña observatory for their effort and dedication in maintaining the instruments. Our colleague Celia Milford has improved the English language of the paper.

References

Angstrom, A.: On the atmospheric transmission of sun radiation and on dust in the air, Geografiska Annaler, 11, 156–166, 1929.

Barreto, A., Cuevas, E., Pallé, P., Romero, P. M., Guirado, C., Wehrli, C. J., and Almansa, F.: Recovering long-term aerosol optical depth series (1976-2012) from an astronomical potassium-based resonance scattering spectrometer, Atmospheric Measurement Techniques, 7, 4103–4116, https://doi.org/10.5194/amt-7-4103-2014, 2014.

Barreto, A., Cuevas, E., Granados-Muñoz, M.-J., Alados-Arboledas, L., Romero, P. M., Gröbner, J., Kouremeti, N., Almansa, A. F., Stone, T., Toledano, C., Román, R., Sorokin, M., Holben, B., Canini, M., and Yela, M.: The new sun-sky-lunar Cimel CE318-T multiband photometer – a comprehensive performance evaluation, Atmospheric Measurement Techniques, 9, 631–654, https://doi.org/10.5194/amt-9-631-2016, https://www.atmos-meas-tech.net/9/631/2016/, 2016.

Basart, S., Pérez, C., Cuevas, E., Baldasano, J. M., and Gobbi, G. P.: Aerosol characterization in Northern Africa, Northeastern Atlantic, Mediterranean Basin and Middle East from direct-sun AERONET observations, Atmospheric Chemistry and Physics, 9, 8265–8282, https://doi.org/10.5194/acp-9-8265-2009, https://www.atmos-chem-phys.net/9/8265/2009/, 2009.

Basart, S., Pérez, C., Nickovic, S., Cuevas, E., and Baldasano, J.: Development and evaluation of the BSC-DREAM8b dust regional model over Northern Africa, the Mediterranean and the Middle East, Tellus B: Chemical and Physical Meteorology, 64, 18 539, https://doi.org/10.3402/tellusb.v64i0.18539, https://doi.org/10.3402/tellusb.v64i0.18539, 2012.

Benedetti, A., Reid, J. S., Knippertz, P., Marsham, J. H., Di Giuseppe, F., Rémy, S., Basart, S., Boucher, O., Brooks, I. M., Menut, L., Mona, L., Laj, P., Pappalardo, G., Wiedensohler, A., Baklanov, A., Brooks, M., Colarco, P. R., Cuevas, E., da Silva, A., Escribano, J., Flemming, J., Huneeus, N., Jorba, O., Kazadzis, S., Kinne, S., Popp, T., Quinn, P. K., Sekiyama, T. T., Tanaka, T., and Terradellas, E.: Status and future of numerical atmospheric aerosol prediction with a focus on data requirements, Atmospheric Chemistry and Physics, 18, 10 615–10 643, https://doi.org/10.5194/acp-18-10615-2018, https://www.atmos-chem-phys.net/18/10615/2018/, 2018.

Blanc, P., Espinar, B., Geuder, N., Gueymard, C., R., M., Pitz-Paal, R., Reinhardt, B., Renné, D., M., S., Wald, L., and Wilbert, S.: Direct normal irradiance related definitions and applications: The circumsolar issue, Solar Energy, 110, 561 – 577, https://doi.org/https://doi.org/10.1016/j.solener.2014.10.001, 2014.

Bodhaine, B. A., Wood, N. B., Dutton, E. G., and Slusser, J. R.: On Rayleigh optical depth calculations, Journal of Atmospheric and Oceanic Technology, 16, 1854–1861, 1999.

Cachorro, V., Toledano, C., Sorribas, M., Berjón, A., De Frutos, A., and Laulainen, N.: An "in situ" calibration-correction procedure (KCICLO) based on AOD diurnal cycle: Comparative results between AERONET and reprocessed (KCICLO method) AOD-alpha data series at El Arenosillo, Spain, Journal of Geophysical Research: Atmospheres, 113, https://doi.org/https://doi.org/10.1029/2007JD009001, 2008.

Cachorro, V. E., Romero, P. M., Toledano, C., Cuevas, E., and de Frutos, A. M.: The fictitious diurnal cycle of aerosol optical depth: A new approach for "in situ" calibration and correction of AOD data series, Geophysical Research Letters, 31, https://doi.org/10.1029/2004GL019651, 2004.

Carrillo, J., Guerra, J. C., and Cuevas, E.and Barrancos, J.: Characterization of the Marine Boundary Layer and the Trade-Wind Inversion over the Sub-tropical North Atlantic, Boundary-Layer Meteorology, 158, 311–330, https://doi.org/10.1007/s10546-015-0081-1, https://doi.org/10.1007/s10546-015-0081-1, 2016.

Chance, K. and Kurucz, R.: An improved high-resolution solar reference spectrum for earth's atmosphere measurements in the ultraviolet, visible, and near infrared, Journal of quantitative spectroscopy and radiative transfer, 111, 1289–1295, https://doi.org/https://doi.org/10.1016/j.jqsrt.2010.01.036, http://www.sciencedirect.com/science/article/pii/S0022407310000610, 2010.

Chedin, A., Capelle, V., and Scott, N.: Detection of IASI dust AOD trends over Sahara: How many years of data required?, Atmospheric Research, 212, 120–129, https://doi.org/https://doi.org/10.1016/j.atmosres.2018.05.004, http://www.sciencedirect.com/science/article/pii/S0169809517310566, 2018.

Chubarova, N. Y., Poliukhov, A. A., and Gorlova, I. D.: Long-term variability of aerosol optical thickness in Eastern Europe over 2001–2014 according to the measurements at the Moscow MSU MO AERONET site with additional cloud and NO_2 correction, Atmospheric Measurement Techniques, 9, 313–334, https://doi.org/10.5194/amt-9-313-2016, https://www.atmos-meas-tech.net/9/313/2016/, 2016.

Cuevas, E., González, Y., Rodríguez, S., Guerra, J. C., Gómez-Peláez, A. J., Alonso-Pérez, S., Bustos, J., and Milford, C.: Assessment of atmospheric processes driving ozone variations in the subtropical North Atlantic free troposphere, Atmospheric Chemistry and Physics, 13, 1973–1998, https://doi.org/10.5194/acp-13-1973-2013, https://www.atmos-chem-phys.net/13/1973/2013/, 2013.

Cuevas, E., Camino, C., Benedetti, A., Basart, S., Terradellas, E., Baldasano, J. M., Morcrette, J. J., Marticorena, B., Goloub, P., Mortier, A., Berjón, A., Hernández, Y., Gil-Ojeda, M., and Schulz, M.: The MACC-II 2007-2008 reanalysis: atmospheric dust evaluation and characterization over northern Africa and the Middle East, Atmospheric Chemistry and Physics, 15, 3991–4024, https://doi.org/10.5194/acp-15-3991-2015, https://www.atmos-chem-phys.net/15/3991/2015/, 2015.

Cuevas, E., Gómez-Peláez, A., Rodríguez, S., Terradellas, E., Basart, S., García, R., García, O., and Alonso-Pérez, S.: The pulsating nature of large-scale Saharan dust transport as a result of interplays between mid-latitude Rossby waves and the North African Dipole Intensity, Atmospheric Environment, 167, 586–602, https://doi.org/https://doi.org/10.1016/j.atmosenv.2017.08.059, http://www.sciencedirect.com/science/article/pii/S1352231017305757, 2017a.

Cuevas, E., Milford, C., Bustos, J. J., del Campo-Hernández, García, O., D., G. R., Gómez-Peláez, Guirado-Fuentes, C., Marrero, C., Prats, N., Ramos, R., Redondas, A., Reyes, E., Rodríguez, S., Romero-Campos, P., Scheneider, M., Belmonte, J., Yela, M., Almansa, F., Barreto, A., López-Solano, C., Basart, S., Terradellas, E., Afonso, S., Bayo, C., Berjón, A., Bethencourt, J., Carreño, V., Castro, N. J., Cruz, A. M., Damas, M., De Ory-Ajamil, F., García, M. I., Gómez-Trueba, V., González, Y., Hernández, C., Hernández, Y., Hernández-Cruz, B., Jover, M., León, S., López-Fernández, R., López-Solano, J., Rodríguez, E., Rodríguez-Franco, J., Rodríguez-Valido, M., Sálamo, C., Sanromá, E., Santana, D., Santo-Tomás, F., Sepúlveda, E., Sierra, M., and Sosa, E.: Izaña Atmospheric Research Center Activity Report 2015-2016, State Meteorological Agency (AEMET), 2017b.

Driemel, A., Augustine, J., Behrens, K., Colle, S., Cox, C., Cuevas-Agulló, E., Denn, F. M., Duprat, T., Fukuda, M., Grobe, H., Haeffelin, M., Hodges, G., Hyett, N., Ijima, O., Kallis, A., Knap, W., Kustov, V., Long, C. N., Longenecker, D., Lupi, A., Maturilli, M., Mimouni, M., Ntsangwane, L., Ogihara, H., Olano, X., Olefs, M., Omori, M., Passamani, L., Pereira, E. B., Schmithüsen, H., Schumacher, S., Sieger, R., Tamlyn, J., Vogt, R., Vuilleumier, L., Xia, X., Ohmura, A., and König-Langlo, G.: Baseline Surface Radiation Network (BSRN): structure and data description (1992–2017), Earth System Science Data, 10, 1491–1501, https://doi.org/10.5194/essd-10-1491-2018, https://www.earth-syst-sci-data.net/10/1491/2018/, 2018.

Dubovik, O., Holben, B., Eck, T. F., Smirnov, A., Kaufman, Y. J., King, M. D., Tanré, D., and Slutsker, I.: Variability of absorption and optical properties of key aerosol types observed in worldwide locations, Journal of the atmospheric sciences, 59, 590–608, https://doi.org/https://doi.org/10.1175/1520-0469(2002)059<0590:VOAAOP>2.0.CO;2, 2002.

Eck, T., Holben, B., Reid, J., Dubovik, O., Smirnov, A., O'neill, N., Slutsker, I., and Kinne, S.: Wavelength dependence of the optical depth of biomass burning, urban, and desert dust aerosols, Journal of Geophysical Research: Atmospheres, 104, 31 333–31 349, https://doi.org/10.1029/1999JD900923, 1999.

Eissa, Y., Blanc, P., Wald, L., and Ghedira, H.: Can AERONET data be used to accurately model the monochromatic beam and circumsolar irradiances under cloud-free conditions in desert environment?, Atmospheric Measurement Techniques, 8, 5099–5112, https://doi.org/DOI = 10.5194/amt-8-5099-2015, 2015.

Eissa, Y., Blanc, P., Ghedira, H., Oumbe, A., and Wald, L.: A fast and simple model to estimate the contribution of the circumsolar irradiance to measured broadband beam irradiance under cloud-free conditions in desert environment, Solar Energy, 163, 497–509, https://doi.org/https://doi.org/10.1016/j.solener.2018.02.015, 2018.

Eskes, H. J. and Boersma, K. F.: Averaging kernels for DOAS total-column satellite retrievals, Atmospheric Chemistry and Physics, 3, 1285–1291, https://doi.org/10.5194/acp-3-1285-2003, https://www.atmos-chem-phys.net/3/1285/2003/, 2003.

García, R. D., Cuevas, E., García, O. E., Cachorro, V. E., Pallé, P., Bustos, J. J., Romero-Campos, P. M., and de Frutos, A. M.: Reconstruction of global solar radiation time series from 1933 to 2013 at the IzaÃ±a Atmospheric Observatory, Atmospheric Measurement Techniques, 7, 3139–3150, https://doi.org/10.5194/amt-7-3139-2014, https://www.atmos-meas-tech.net/7/3139/2014/, 2014.

García, R. D., Barreto, A., Cuevas, E., Gröbner, J., García, O. E., Gómez-Peláez, A., Romero-Campos, P. M., Redondas, A., Cachorro, V. E., and Ramos, R.: Comparison of observed and modeled cloud-free longwave downward radiation (2010–2016) at the high mountain BSRN Izaña station, Geoscientific Model Development, 11, 2139–2152, https://doi.org/10.5194/gmd-11-2139-2018, https://www.geosci-model-dev.net/11/2139/2018/, 2018.

Ge, J., Su, J., Fu, Q., Ackerman, T., and Huang, J.: Dust aerosol forward scattering effects on ground-based aerosol optical depth retrievals, Journal of Quantitative Spectroscopy and Radiative Transfer, 112, 310–319, https://doi.org/https://doi.org/10.1016/j.jqsrt.2010.07.006, 2011.

Giles, D. M., Sinyuk, A., Sorokin, M. S., Schafer, J. S., Smirnov, A., Slutsker, I., Eck, T. F., Holben, B. N., Lewis, J., Campbell, J., Welton, E. J., Korkin, S., and Lyapustin, A.: Advancements in the Aerosol Robotic Network (AERONET) Version 3 Database – Automated Near Real-Time Quality Control Algorithm with Improved Cloud Screening for Sun Photometer Aerosol Optical Depth (AOD) Measurements, Atmospheric Measurement Techniques Discussions, 2018, 1–78, https://doi.org/10.5194/amt-2018-272, https://www.atmos-meas-tech-discuss.net/amt-2018-272/, 2018.

Goloub, P., Li, Z., Dubovik, O., Blarel, L., Podvin, T., Jankowiak, I., Lecoq, R., Deroo, C., Chatenet, B., Morel, J., Cuevas, E., and Ramos, R.: PHOTONS/AERONET sunphotometer network overview: description, activities, results, in: Fourteenth International Symposium on Atmospheric and Ocean Optics/Atmospheric Physics, vol. 6936, p. 69360V, International Society for Optics and Photonics, 2007.

Gueymard, C.: SMARTS2: a simple model of the atmospheric radiative transfer of sunshine: algorithms and performance assessment, Florida Solar Energy Center Cocoa, FL, 1995.

Gueymard, C.: Parameterized transmittance model for direct beam and circumsolar spectral irradiance, Solar Energy, 71, 325–346, https://doi.org/https://doi.org/10.1016/S0038-092X(01)00054-8, http://www.sciencedirect.com/science/article/pii/S0038092X01000548, 2001.

Guirado, C., Cuevas, E., Cachorro, V. E., Toledano, C., Alonso-Pérez, S., Bustos, J. J., Basart, S., Romero, P. M., Camino, C., Mimouni, M., Zeudmi, L., Goloub, P., Baldasano, J. M., and de Frutos, A. M.: Aerosol characterization at the Saharan AERONET site Tamanrasset, Atmospheric Chemistry and Physics, 14, 11 753–11 773, https://doi.org/10.5194/acp-14-11753-2014, https://www.atmos-chem-phys.net/14/11753/2014/, 2014.

Holben, B., Eck, T., Slutsker, I., Tanré, D., Buis, J., Setzer, A., Vermote, E., Reagan, J., and Kaufman, Y.: Multi-band automatic sun and sky scanning radiometer system for measurement of aerosols, pp. 75–83, CNES, Proceedings of 6th International Symposium on Physical Measurements and Signatures in Remote Sensing, 1994.

Holben, B., Eck, T., Slutsker, I., Tanré, D., Buis, J., Setzer, A., Vermote, E., Reagan, J., Kaufman, Y., Nakajima, T., Lavenu, F., Jankowiak, I., and Smirnov, A.: AERONET—A Federated Instrument Network and Data Archive for Aerosol Characterization, Remote Sensing of Environment, 66, 1 – 16, https://doi.org/https://doi.org/10.1016/S0034-4257(98)00031-5, 1998.

Holben, B., Tanre, D., Smirnov, A., Eck, T., Slutsker, I., Abuhassan, N., Newcomb, W., Schafer, J., Chatenet, B., Lavenu, F., et al.: An emerging ground-based aerosol climatology: Aerosol optical depth from AERONET, Journal of Geophysical Research: Atmospheres, 106, 12 067–12 097, https://doi.org/https://doi.org/10.1029/2001JD900014, 2001.

Huijnen, V. and Eskes, H.: Skill scores and evaluation methodology for the MACC II project, MACC-II Deliverable D_85, 2, http://www.gmes-atmosphere.eu/documents/maccii/deliverables/val/MACCII_VAL_DEL_D_85.2_ScoringReport01_20120222.pdf, 2012.

Huneeus, N., Basart, S., Fiedler, S., Morcrette, J.-J., Benedetti, A., Mulcahy, J., Terradellas, E., Pérez García-Pando, C., Pejanovic, G., Nickovic, S., Arsenovic, P., Schulz, M., Cuevas, E., Baldasano, J. M., Pey, J., Remy, S., and Cvetkovic, B.: Forecasting the northern African dust outbreak towards Europe in April 2011: a model intercomparison, Atmospheric Chemistry and Physics, 16, 4967–4986, https://doi.org/10.5194/acp-16-4967-2016, https://www.atmos-chem-phys.net/16/4967/2016/, 2016.

IPCC: The Physical Science Basis. Intergovernmental Panel on Climate Change, https://doi.org/doi:10.1017/CBO9781107415324, 2013.

Kahn, R. A. and Gaitley, B. J.: An analysis of global aerosol type as retrieved by MISR, Journal of Geophysical Research: Atmospheres, 120, 4248–4281, https://doi.org/10.1002/2015JD023322, https://agupubs.onlinelibrary.wiley.com/doi/abs/10.1002/2015JD023322, 2015.

Kalnay, E., Kanamitsu, M., Kistler, R., Collins, W., Deaven, D., Gandin, L., Iredell, M., Saha, S., White, G., Woollen, J., et al.: The NCEP/NCAR 40-year reanalysis project, Bulletin of the American meteorological Society, 77, 437–472, 1996.

Kasten, F.: A new table and approximation formula for the relative optical air mass, Archiv für Meteorologie, Geophysik und Bioklimatologie, Serie B, 14, 206–223, https://doi.org/https://doi.org/10.1007/BF02248840, 1966.

Kasten, F. and Young, A. T.: Revised optical air mass tables and approximation formula, Appl. Opt., 28, 4735–4738, https://doi.org/10.1364/AO.28.004735, 1989.

Kazadzis, S., Veselovskii, I., Amiridis, V., Gröbner, J., Suvorina, A., Nyeki, S., Gerasopoulos, E., Kouremeti, N., Taylor, M., Tsekeri, A., and Wehrli, C.: Aerosol microphysical retrievals from precision filter radiometer direct solar radiation measurements and comparison with AERONET, Atmospheric Measurement Techniques, 7, 2013–2025, https://doi.org/10.5194/amt-7-2013-2014, https://www.atmos-meas-tech.net/7/2013/2014/, 2014.

Kazadzis, S., Kouremeti, N., Diémoz, H., Gröbner, J., Forgan, B. W., Campanelli, M., Estellés, V., Lantz, K., Michalsky, J., Carlund, T., Cuevas, E., Toledano, C., Becker, R., Nyeki, S., Kosmopoulos, P. G., Tatsiankou, V., Vuilleumier, L., Denn, F. M., Ohkawara, N., Ijima, O., Goloub, P., Raptis, P. I., Milner, M., Behrens, K., Barreto, A., Martucci, G., Hall, E., Wendell, J., Fabbri, B. E., and Wehrli, C.: Results from the Fourth WMO Filter Radiometer Comparison for aerosol optical depth measurements, Atmospheric Chemistry and Physics, 18, 3185–3201, https://doi.org/10.5194/acp-18-3185-2018, 2018a.

Kazadzis, S., Kouremeti, N., Nyeki, S., Gröbner, J., and Wehrli, C.: The World Optical Depth Research and Calibration Center (WORCC) quality assurance and quality control of GAW-PFR AOD measurements, Geoscientific Instrumentation, Methods and Data Systems, 7, 39–53, https://doi.org/10.5194/gi-7-39-2018, https://www.geosci-instrum-method-data-syst.net/7/39/2018/, 2018b.

Kim, S.-W., Jefferson, A., Soon-Chang, Y., Dutton, E., Ogren, J., Valero, F., Kim, J., and Holben, B.: Comparisons of aerosol optical depth and surface shortwave irradiance and their effect on the aerosol surface radiative forcing estimation, Journal of Geophysical Research: Atmospheres, 110, https://doi.org/10.1029/2004JD004989, 2005.

Kim, S.-W., Yoon, S.-C., Kim, J., and Kim, S.-Y.: Seasonal and monthly variations of columnar aerosol optical properties over east Asia determined from multi-year MODIS, LIDAR, and AERONET Sun/sky radiometer measurements, Atmospheric Environment, 41, 1634–1651, https://doi.org/https://doi.org/10.1016/j.atmosenv.2006.10.044, 2007.

Kim, S.-W., Yoon, S.-C., Dutton, E., Kim, J., and Wehrli, C.and Holben, B.: Global surface-based sun photometer network for long-term observations of column aerosol optical properties: intercomparison of aerosol optical depth, Aerosol Science and Technology, 42, 1–9, https://doi.org/https://doi.org/10.1080/02786820701699743, 2008.

Klingmüller, K., Pozzer, A., Metzger, S., Stenchikov, G. L., and Lelieveld, J.: Aerosol optical depth trend over the Middle East, Atmospheric Chemistry and Physics, 16, 5063–5073, https://doi.org/10.5194/acp-16-5063-2016, 2016.

Komhyr, W.: Dobson spectrophotometer systematic total ozone measurement error, Geophysical Research Letters, 7, 161–163, 1980.

Komhyr, W. D., Grass, R. D., and Leonard, R. K.: Dobson spectrophotometer 83: A standard for total ozone measurements, 1962–1987, Journal of Geophysical Research: Atmospheres, 94, 9847–9861, https://doi.org/10.1029/JD094iD07p09847, 1989.

McArthur, L. J. B., Halliwell, D. H., Niebergall, O. J., O'Neill, N. T., Slusser, J. R., and Wehrli, C.: Field comparison of network Sun photometers, Journal of Geophysical Research: Atmospheres, 108, https://doi.org/10.1029/2002JD002964, 2003.

McPeters, R., Frith, S., and Labow, G.: OMI total column ozone: extending the long-term data record, Atmospheric Measurement Techniques, 8, 4845–4850, https://doi.org/https://doi.org/10.5194/amt-8-4845-2015, 2015.

Mitchell, R. and Forgan, B.: Aerosol measurement in the Australian outback: Intercomparison of sun photometers, Journal of Atmospheric and Oceanic Technology, 20, 54–66, https://doi.org/https://doi.org/10.1175/1520-0426(2003)020<0054:AMITAO>2.0.CO;2, 2003.

Nyeki, S., Halios, C., Baum, W., Eleftheriadis, K., Flentje, H., Gröbner, J., Vuilleumier, L., and Wehrli, C.: Ground-based aerosol optical depth trends at three high-altitude sites in Switzerland and southern Germany from 1995 to 2010, Journal of Geophysical Research: Atmospheres, 117, https://doi.org/https://doi.org/10.1029/2012JD017493, 2012.

Nyeki, S., Gröbner, J., and Wehrli, C.: Ground-based aerosol optical depth inter-comparison campaigns at European EUSAAR super-sites, vol. 1531, pp. 584–587, https://doi.org/10.1063/1.4804837, 2013.

Nyeki, S., Wehrli, C., Gröbner, J., Kouremeti, N., Wacker, S., Labuschagne, C., Mbatha, N., and Brunke, E.-G.: The GAW-PFR aerosol optical depth network: The 2008–2013 time series at Cape Point Station, South Africa, Journal of Geophysical Research: Atmospheres, 120, 5070–5084, 2015.

Rodríguez, S., González, Y., Cuevas, E., Ramos, R., Romero, P. M., Abreu-Afonso, J., and Redondas, A.: Atmospheric nanoparticle observations in the low free troposphere during upward orographic flows at IzaÃ±a Mountain Observatory, Atmospheric Chemistry and Physics, 9, 6319–6335, https://doi.org/10.5194/acp-9-6319-2009, 2009.

Rodríguez, S., Alastuey, A., Alonso-Pérez, S., Querol, X., Cuevas, E., Abreu-Afonso, J., Viana, M., Pérez, N., Pandolfi, M., and de la Rosa, J.: Transport of desert dust mixed with North African industrial pollutants in the subtropical Saharan Air Layer, Atmospheric Chemistry and Physics, 11, 6663–6685, https://doi.org/10.5194/acp-11-6663-2011, 2011.

Rodríguez, S., Cuevas, E., Prospero, J. M., Alastuey, A., Querol, X., López-Solano, J., García, M. I., and Alonso-Pérez, S.: Modulation of Saharan dust export by the North African dipole, Atmospheric Chemistry and Physics, 15, 7471–7486, https://doi.org/10.5194/acp-15-7471-2015, 2015.

Romero, P. M. and Cuevas, E.: Variación diurna del espesor óptico de aerosoles:¿ ficción o realidad?, 3 Asamblea Hispano Portuguesa de Geofísica y Geodesia. Valencia, 2002.

Romero-Campos, P., Cuevas, A., Kazadzis, S., Kouremeti, N., García, R., and Guirado-Fuentes, C.: Análisis de la trazabilidad en los valores del AOD obtenidos a partir de las medidas de las redes AERONET-CIMEL y GAW-PFR durante el período 2005-2015 en el Observatorio Atmosférico de Izaña, 2017.

Sayer, A. M., Hsu, N. C., Bettenhausen, C., Jeong, M., Holben, B. N., and Zhang, J.: Global and regional evaluation of over-land spectral aerosol optical depth retrievals from SeaWiFS, Atmospheric Measurement Techniques, 5, 1761–1778, https://doi.org/10.5194/amt-5-1761-2012, 2012.

Sayer, A. M., Hsu, N. C., Bettenhausen, C., and Jeong, M.: Validation and uncertainty estimates for MODIS Collection 6 "Deep Blue" aerosol data, Journal of Geophysical Research: Atmospheres, 118, 7864–7872, https://doi.org/10.1002/jgrd.50600, https://agupubs.onlinelibrary.wiley.com/doi/abs/10.1002/jgrd.50600, 2013.

Schmid, B. and Wehrli, C.: Comparison of Sun photometer calibration by use of the Langley technique and the standard lamp, Appl. Opt., 34, 4500–4512, https://doi.org/10.1364/AO.34.004500, http://ao.osa.org/abstract.cfm?URI=ao-34-21-4500, 1995.

Schmid, B., Michalsky, J., Halthore, R., Beauharnois, M., Harrison, L., Livingston, J., Russell, P., Holben, B., Eck, T., and Smirnov, A.: Comparison of aerosol optical depth from four solar radiometers during the fall 1997 ARM intensive observation period, Geophysical Research Letters, 26, 2725–2728, https://doi.org/10.1029/1999GL900513, https://agupubs.onlinelibrary.wiley.com/doi/abs/10.1029/1999GL900513, 1999.

Smirnov, A., Holben, B., Eck, T., Dubovik, O., and Slutsker, I.: Cloud-screening and quality control algorithms for the AERONET database, Remote sensing of environment, 73, 337–349, https://doi.org/https://doi.org/10.1016/S0034-4257(00)00109-7, http://www.sciencedirect.com/science/article/pii/S0034425700001097, 2000.

Todd, M. C., Washington, R., Martins, J. V., Dubovik, O., Lizcano, G., M'bainayel, S., and Engelstaedter, S.: Mineral dust emission from the Bodélé Depression, northern Chad, during BoDEx 2005, Journal of Geophysical Research: Atmospheres, 112, https://doi.org/https://doi.org/10.1029/2006JD007170, 2007.

Toledano, C., Cachorro, V. E., Berjón, A., de Frutos, A. M., Sorribas, M., de la Morena, B. A., and Goloub, P.: Aerosol optical depth and Ångström exponent climatology at El Arenosillo AERONET site (Huelva, Spain), Quarterly Journal of the Royal Meteorological Society, 133, 795–807, https://doi.org/10.1002/qj.54, https://rmets.onlinelibrary.wiley.com/doi/abs/10.1002/qj.54, 2007.

Toledano, C., Cachorro, V., Gausa, M., Stebel, K., Aaltonen, V., Berjón, A., de Galisteo, J. P. O., de Frutos, A. M., Bennouna, . Y., Blindheim, S., Myhre, C. L., Zibordi, G., Wehrli, C., Kratzer, S., Hakansson, B., Carlund, T., de Leeuw, G., Herber, A., and Torres, B.: Overview of Sun Photometer Measurements of Aerosol Properties in Scandinavia and Svalbard, Atmospheric Environment, 52, 18–28, https://doi.org/10.1016/j.atmosenv.2011.10.022, 2012.

Toledano, C., González, R., Fuertes, D., Cuevas, E., Eck, T. F., Kazadzis, S., Kouremeti, N., Gröbner, J., Goloub, P., Blarel, L., Román, R., Barreto, A., Berjón, A., Holben, B. N., and Cachorro, V. E.: Assessment of Sun photometer Langley calibration at the high-elevation sites Mauna Loa and Izaña, Atmospheric Chemistry and Physics, 18, 14 555–14 567, https://doi.org/10.5194/acp-18-14555-2018, 2018.

Torres, B., Toledano, C., Berjón, A., Fuertes, D., Molina, V., Gonzalez, R., Canini, M., Cachorro, V. E., Goloub, P., Podvin, T., Blarel, L., Dubovik, O., Bennouna, Y., and de Frutos, A. M.: Measurements on pointing error and field of view of Cimel-318 Sun photometers in the scope of AERONET, Atmospheric Measurement Techniques, 6, 2207–2220, https://doi.org/10.5194/amt-6-2207-2013, 2013.

Wagner, F. and Silva, A. M.: Some considerations about Angström exponent distributions, Atmospheric Chemistry and Physics, 8, 481–489, https://doi.org/10.5194/acp-8-481-2008, 2008.

Wang, J., Xia, X., Wang, P., and Christopher, S.: Diurnal variability of dust aerosol optical thickness and Ångström exponent over dust source regions in China, Geophysical Research Letters, 31, https://doi.org/10.1029/2004GL019580, https://agupubs.onlinelibrary.wiley.com/doi/abs/10.1029/2004GL019580, 2004.

Wehrli, C.: Calibrations of filter radiometers for determination of atmospheric optical depth, Metrologia, 37, 419, http://stacks.iop.org/0026-1394/37/i=5/a=16, 2000.

Wehrli, C.: GAWPFR: A network of aerosol optical depth observations with precision filter radiometers, GLOBAL ATMOSPHERE WATCH, p. 36, 2005.

Wehrli, C.: Precision Filter Radiometer Documentation,Version 4.0, 38 pp.,Davos Dorf, 2008a.

Wehrli, C.: Remote sensing of aerosol optical depth in a global surface network, Ph.D. thesis, ETH Zurich, https://www.research-collection.ethz.ch/bitstream/handle/20.500.11850/150574/eth-30693-02.pdf, 2008b.

Wilbert, S.: Determination of circumsolar radiation and its effect on concentrating solar power, Ph.D. thesis, Hochschulbibliothek der Rheinisch-Westfälischen Technischen Hochschule Aachen, https://d-nb.info/1059537710/34, 2014.

WMO: Aerosol measurement procedures, guidelines and recommendations, GAW Report No. 153, WMO TD No. 1178, https://library.wmo.int/pmb_ged/wmo-td_1178.pdf, 2003.

WMO: WMO/GAW Experts Workshop on a Global Surface-Based Network for Long Term Observations of Column Aerosol Optical Properties,GAW Report No. 162, WMO TD No. 1287, https://library.wmo.int/pmb_ged/wmo-td_1287.pdf, 2005.

WMO: Abridged final report with resolutions and recommendations ,GAW Report WMO TD No. 1019,WMO-CIMO Fourteenth session Geneva 7–14 December 2006, 2007.

Young, A. T.: Revised depolarization corrections for atmospheric extinction, Appl. Opt., 19, 3427–3428, https://doi.org/10.1364/AO.19.003427, 1980.